






Article

Monitoring Bacterial Community Dynamics in a Drinking Water Treatment Plant: An Integrative Approach Using Metabarcoding and Microbial Indicators in Large Water Volumes

Anna Pinar-Méndez ^{1,2,3,*} , Owen S. Wangensteen ⁴ , Kim Præbel ⁴ , Belén Galofré ¹, Javier Méndez ² , Anicet R. Blanch ^{2,3}  and Cristina García-Aljaro ^{2,3,*}

- ¹ Aigües de Barcelona, Empresa Metropolitana de Gestió del Cicle Integral de l'Aigua, 08028 Barcelona, Spain; bgalofre@aiguesdebarcelona.cat
- ² Department of Genetics, Microbiology and Statistics, Faculty of Biology, University of Barcelona, 08028 Barcelona, Spain; jmendez@ub.edu (J.M.); ablanch@ub.edu (A.R.B.)
- ³ The Water Research Institute, University of Barcelona, 08001 Barcelona, Spain
- ⁴ Norwegian College of Fishery Science, Faculty of Biosciences, Fisheries and Economics, UiT The Arctic University of Norway, N-9037 Tromsø, Norway; owen.wangensteen@uit.no (O.S.W.); kim.praebel@uit.no (K.P.)
- * Correspondence: apinar@aiguesdebarcelona.cat (A.P.-M.); crgarcia@ub.edu (C.G.-A.); Tel.: +34-93-247-98-12 (A.P.-M.); +34-93-402-14-84 (C.G.-A.)



Citation: Pinar-Méndez, A.; Wangensteen, O.S.; Præbel, K.; Galofré, B.; Méndez, J.; Blanch, A.R.; García-Aljaro, C. Monitoring Bacterial Community Dynamics in a Drinking Water Treatment Plant: An Integrative Approach Using Metabarcoding and Microbial Indicators in Large Water Volumes. *Water* **2022**, *14*, 1435. <https://doi.org/10.3390/w14091435>

Academic Editor: Anas Ghadouani

Received: 17 February 2022

Accepted: 28 April 2022

Published: 30 April 2022

Publisher's Note: MDPI stays neutral with regard to jurisdictional claims in published maps and institutional affiliations.



Copyright: © 2022 by the authors. Licensee MDPI, Basel, Switzerland. This article is an open access article distributed under the terms and conditions of the Creative Commons Attribution (CC BY) license (<https://creativecommons.org/licenses/by/4.0/>).

Abstract: Monitoring bacterial communities in a drinking water treatment plant (DWTP) may help to understand their regular operations. Bacterial community dynamics in an advanced full-scale DWTP were analyzed by 16S rRNA metabarcoding, and microbial water quality indicators were determined at nine different stages of potabilization: river water and groundwater intake, decantation, sand filtration, ozonization, carbon filtration, reverse osmosis, mixing chamber and post-chlorination drinking water. The microbial content of large water volumes (up to 1100 L) was concentrated by hollow fiber ultrafiltration. Around 10 million reads were obtained and grouped into 10,039 amplicon sequence variants. Metabarcoding analysis showed high bacterial diversity at all treatment stages and above all in groundwater intake, followed by carbon filtration and mixing chamber samples. Shifts in bacterial communities occurred downstream of ozonization, carbon filtration, and, more drastically, chlorination. Proteobacteria and Bacteroidota predominated in river water and throughout the process, but in the final drinking water, the strong selective pressure of chlorination reduced diversity and was clearly dominated by Cyanobacteria. Significant seasonal variation in species distribution was observed in decantation and carbon filtration samples. Some amplicon sequence variants related to potentially pathogenic genera were found in the DWTP. However, they were either not detected in the final water or in very low abundance (<2%), and all EU Directive quality standards were fully met. A combination of culture and high-throughput sequencing techniques may help DWTP managers to detect shifts in microbiome, allowing for a more in-depth assessment of operational performance.

Keywords: water quality monitoring; drinking water treatment plant; drinking water; 16S rRNA metabarcoding; amplicon sequencing; hollow fiber ultrafiltration; bacterial diversity

1. Introduction

Freshwater resources are particularly vulnerable to the consequences of climate change. A general increase in temperature can promote eutrophication of surface waters [1,2], whereas more frequent extreme weather events, such as heavy rainstorms and longer drought periods, may impact the availability of safe drinking water, especially in water-stressed regions such as the Mediterranean. Temperature is a crucial determinant of water quality, since it influences microbial dynamics such as uncontrolled proliferation that can

facilitate biofilm formation [3,4]. In a global warming scenario where water temperature is expected to rise, a potential change in microbial biodiversity can occur and can involve the emergence of some opportunistic bacteria in drinking water [3].

Pressures on water resources and quality are further exacerbated by the growing concentration of human populations in metropolitan areas and intensification of industrial activities [5]. In such a scenario, the provision of sufficient safe water for all citizens is an increasing challenge for water production management at drinking water treatment plants (DWTP).

The aim of a DWTP is to bring source water up to established drinking water quality standards by removing organic materials and pathogens and by reducing the total bacteria, with or without residual disinfectants. Current regulations to guarantee the safety of water for human consumption are still focused on monitoring culturable fecal indicators and heterotrophic bacteria plate counts (HPC). Although the European Directive (EU) 2020/2184 states that drinking water must be free of the fecal indicators *Escherichia coli* and intestinal enterococci, it does not stipulate upper limits for HPC but rather only the absence of abnormal changes; thus, each member state is responsible for defining a threshold for what constitutes an acceptable level of change. That minimum change in microbial water quality is defined as biological stability [6], and the aim is to provide drinking water to consumers with the same quality achieved in DWTPs. However, unwanted changes may occur during operational procedures or in distribution networks, and studies have shown that, during the potabilization process, water with a stable HPC may have a variable microbial composition and abundance that is undetectable by conventional methods [7–9]. Moreover, the water microbiome may contain opportunistic pathogens and other underexplored diversity. Therefore, alternative approaches are needed for a better understanding of microbiomes in water systems to improve water management from source to tap.

High-throughput sequencing techniques, such as 16S rRNA metabarcoding, have the potential to provide in-depth information that complements standard bacterial quality parameters, and they can help to generate a more accurate picture of microbial communities at different water treatment stages. Several water microbiome studies based on 16S rRNA amplicon sequencing have described microbial composition in DWTPs and distribution networks, which differs according to the water source (e.g., river [10–14], lake [15], groundwater [13,16] or seawater [17]).

A critical parameter in water quality monitoring is the sampling procedure, which needs to ensure the integrity and representativeness of the sampled water. Analyzing large volumes can be an effective approach to detect low-concentration targets. In recent years, dead-end ultrafiltration (DEUF) using hollow fiber filters has emerged as an effective sampling technique based on size exclusion, allowing for good simultaneous recoveries of bacteria, viruses and protozoa from large volumes of water (up to 1100 L) [18–20]. Advantages of using DEUF methods include an all-in-one concentrating procedure for microbes; an improved sample representativity (in comparison with conventional small-volume concentration methods); and the ability to detect low numbers of microbes, including biothreat agents [21], waterborne pathogens [19,22,23] or indicators [24] in large-volume water samples without filter clogging. However, very few studies have applied this method to study microbial biodiversity in the field of water, and they have been mainly focused on distribution networks [8,25,26]. To the best of our knowledge, this is the first study of a full-scale DWTP using 16S rRNA metabarcoding with hollow fiber ultrafiltration methods.

The main goal of this work is to assess the effects of different treatment stages on bacterial communities in a full-scale DWTP. By combining conventional microbial water quality analysis based on the European Directive (EU) 2020/2184 with 16S rRNA metabarcoding, we hope to achieve a more in-depth description of the microbial baseline in the DWTP to evaluate process performance and for the detection of process instability.

2. Materials and Methods

2.1. Sample Collection

The study was carried out in a full-scale DWTP in Sant Joan Despí, Barcelona (Catalonia, northeastern Spain) between 2018 and 2019. This large supply system, located in the lower Llobregat River Basin, has an average production capacity of $\sim 345,000 \text{ m}^3$ a day, which provides drinking water to more than 3.2 million inhabitants in the Barcelona metropolitan area. The complexity of the treatment applied is determined by distinctive features, such as scarcity of water resources ($22 \text{ m}^3/\text{s}$ average flow rate), irregular Mediterranean-type rainfall (from drought to flood) and the influence of industrial and agriculture activities upstream, including potash mining and wastewater treatment plants, on raw water quality (Figure 1). In summary, the plant has two sources of water (river and groundwater). Surface water from the Llobregat River is pumped into the DWTP and cleaned of sand and gravel, before undergoing sequential treatments. The pretreatment stages consist of coagulation/flocculation of organic matter and an initial disinfection with chlorine dioxide, followed by decantation to eliminate flocculants. Subsequently, sand filtration is performed to retain smaller particles held in suspension. The pretreated water then converges with groundwater intake, and both are pumped into two independent treatment lines: one based on conventional processes of ozonization and filtration by granular activated carbon, and the other based on advanced treatments, namely, ultrafiltration, reverse osmosis and remineralization. The water from both lines is mixed in a chamber and stabilized, and then it is treated with chlorine ($0.5\text{--}1.5 \text{ mg/L}$ residual chlorine) in a separated tank before being pumped into the distribution network.

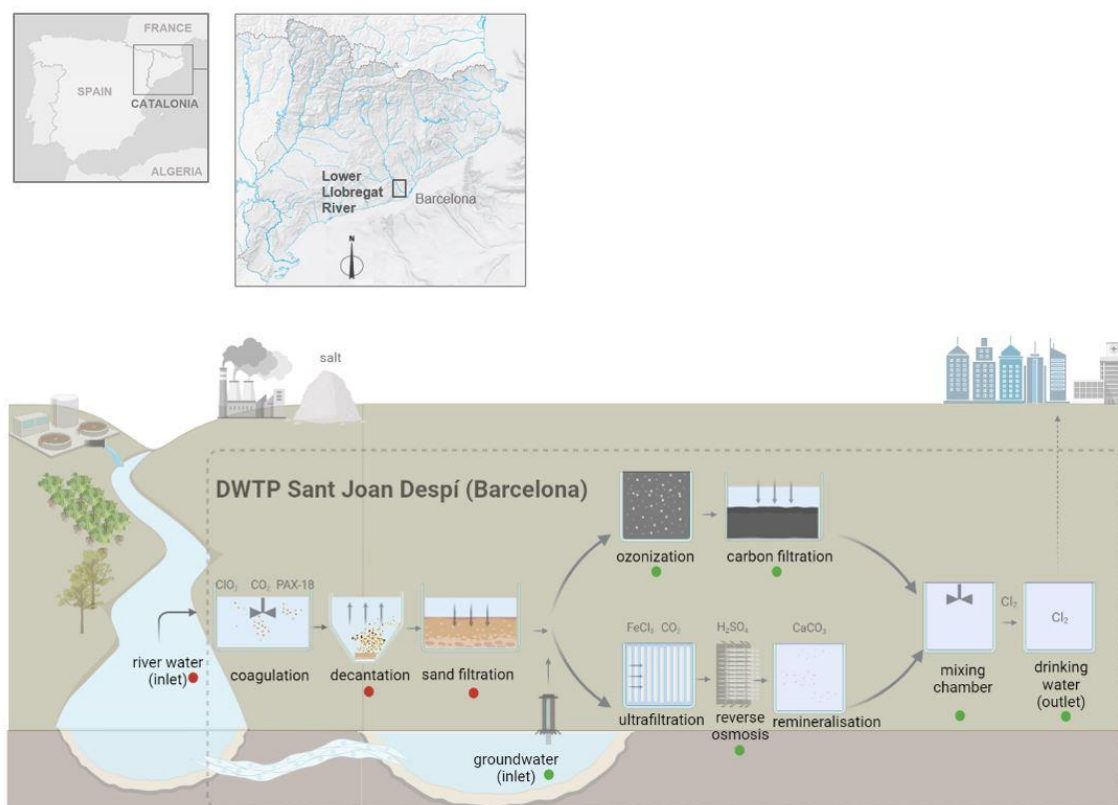


Figure 1. Study site in the lower Llobregat River and schematic diagram of DWTP stages in Sant Joan Despí (Barcelona Spain). Sites of sample collection for this study are indicated with a red spot (high microbial load) and green spot (lower microbial load). Physical map of Catalan hydrographic basins was made by Institut Cartogràfic and Geològic de Catalunya (ICGC).

Eight sampling campaigns were carried out over one year, covering seasons of high and low temperatures and avoiding big rainfall episodes, as the aim was to determine bacterial populations under usual DWTP operative conditions.

A total of 72 water samples were collected at nine different stages of treatment of the DWTP (Figure 1): river water (RW, $n = 8$) and groundwater (GW, $n = 8$) intake, decantation (DEC, $n = 8$), sand filtration (SF, $n = 8$), ozonization (OZ, $n = 8$), carbon filtration (CF, $n = 8$), reverse osmosis (RO, $n = 8$), mixed chamber (MIX, $n = 8$) and post-chlorinated water (DW, $n = 8$). Sampling sites were classified into two groups according to microbial load: river water and pretreatment stages (RW, DEC, SF) (high microbial load), and groundwater and conventional/advanced treatments (GW, OZ, CF, RO, MIX, DW) (lower microbial load). Sampling and processing conditions were different for each group, as described below.

For the first group (pretreatment stages), 2 L of water was collected in polyethylene sterile bottles with sodium thiosulfate (24 mg/L). For the second group (treatment stages), higher volumes were sampled (from 100 to 1100 L/sample) by dead-end hollow fiber ultrafiltration (DEUF) [18–20] using Rexeed™ 25-A filters (Asahi Kasei Medical Co, Tokyo, Japan) of 30 KDa size exclusion. The sampling procedure took several hours (2 to 8.5 h). Chlorinated samples were pretreated with sodium thiosulfate (24 mg/L). All samples were transported to the laboratory at 4 °C for further analyses within 24 h.

Surface Water Contamination Episode and Changes in Operational Procedures

One additional sampling campaign was carried out during a contamination episode affecting the Llobregat River, which forced the DWTP to change its routine operational conditions. The contamination was due to the leakage of brine from a 120 km-long collector that runs parallel to the river and discharges brine produced by potash mining upstream into the sea (for more information about the collector, see Martin-Alonso [27]). To prevent this pollution spill from entering the DWTP, the RW intake was stopped, and the DWTP continued operating only with GW, which does not undergo any of the pre-treatments. The water was treated with CF and chlorination but not with OZ, which was stopped to reduce subproduct bromate formation, nor with RO, as this process produces brine and is discharged into the same collector, which needed to be empty for the required repair. Sampling was carried out at two sites, GW ($n = 1$) and CF ($n = 1$), four days after the DWTP had changed to these operating conditions. Microbial water quality parameters were also analyzed.

2.2. Sample Processing and Nucleic Acid Extraction

For the first group (pretreatment stages), different volumes of water were filtered through 0.22 µm polycarbonate membranes (Millipore, Molsheim, Alsace, France): RW (250 mL), DEC (500 mL–750 mL) and SF (750 mL–1 L). Each filter was placed face down in a sterile flask containing 5 mL of Ringer's solution 1:4 and was eluted by sonication (40 kHz) for 4 min in a Branson Ultrasonics CPX 3800 h ultrasonic water bath (Fischer Scientific, Madrid, Spain), keeping the sample on ice to avoid overheating, and then the sample was vortexed for 1 min. The resulting eluate (ca. 5 mL), containing biomass detached from the membrane, was used for genomic DNA extraction. The remaining original sample was used to determine culturable microbial indicators.

For the second group (treatment stages), water samples were concentrated by Rexeed filters and were eluted in the backflush mode using a peristaltic pump at 1 L/min and 500 mL of phosphate-buffered saline solution (0.5 mL of 1% Antifoam (Sigma-Aldrich, Saint Louis, MO, USA), 10% Tween 80 (Scharlab, Sentmenat, Barcelona, Spain) and 0.5 mL of 10% NaPP (Sigma-Aldrich, Saint Louis, MO, USA)). The Rexeed eluate volume of 500–650 mL was divided to be used for different purposes: a total of 120–170 mL was kept for the culture-based analysis, and the remaining volume (or until filter clogging) was further reduced by centrifugation at $3500 \times g$ using Centricon®70 plus (Merck, Darmstadt Germany) to a 2–4 mL concentrate for nucleic acid extraction.

DNA from samples was extracted using the automated MagNA Pure LC DNA Isolation Kit III (Bacteria, Fungi) (Roche Diagnostics GmbH, Mannheim, Germany), as described below. To obtain a maximum DNA yield, pre-isolation and external lysis steps were applied prior to extraction to reduce eluate volumes. Sample eluates (2 mL) were centrifuged for 10 min at $8000\times g$ at $4\text{ }^{\circ}\text{C}$, and the supernatants were discarded. After the addition of a premixed lysis buffer (130 μL) (Roche Diagnostics GmbH, Germany) and proteinase K (20 μL) (Roche Diagnostics GmbH, Germany), the sample was incubated for 10 min at $65\text{ }^{\circ}\text{C}$. To enhance cell lysis and inactivate potentially pathogenic organisms in the sample, a boiling step was performed, in which the samples were heated at $95\text{ }^{\circ}\text{C}$ for 10 min and then cooled on ice for 1 min.

For sample eluates with high viscosity or large pellets, additional steps were carried out, as recommended by the manufacturer. In summary, mechanical homogenization was performed to enhance lysis of bacterial cells, in which up to 0.40 g of 0.5 mm-diameter silica glass beads (Sigma-Aldrich, Saint Louis, MO, USA) were transferred to the sample tubes. Samples were homogenized by vortexing for 30 s and cooled for 1 min in a cooling block. The samples were then centrifuged for 5 min at $17,000\times g$, and the supernatant was placed in an Eppendorf tube to undergo the same pre-isolation steps as the other samples described above, except for the first centrifugation.

After the pre-isolation protocol, samples were transferred into the sample cartridge for automatic nucleic acid extraction. DNA quality was verified by visualization on 0.8% agarose electrophoresis gel, and the concentration was measured with a Qubit dsDNA HS Assay Kit on a Qubit 3.0 Fluorometer (Invitrogen, Waltham, MA, USA).

2.3. Microbial Water Quality Analysis

All samples were processed within 12 h of collection and were processed for microbial water quality according to the European Directive (EU) 2020/2184 [28], which is based on the analysis of culturable bacterial indicators and heterotrophic bacteria.

The heterotrophic bacteria were cultured by mass inoculation according to the ISO Standard 6222:1999 [29]. Different sample volumes (0.001–1 mL) were inoculated in duplicate in ISO Water Plate Count Agar (WPCA) (Oxoid, Basingstoke, UK) at $22\pm 2\text{ }^{\circ}\text{C}$ for $72\text{ h}\pm 3\text{ h}$.

The enumeration of culturable total coliform bacteria and *E. coli* based on the ISO Standard 9308-2:2012 [30] was performed simultaneously using a Colilert 18[®] test kit and a Quanti-Tray[®]/2000 (Idexx, Westbrook, ME, USA) with 100 mL sample volumes. Only for river water, samples were diluted 1/10 and 1/100. After being transferred to the Quanti-Tray/2000 blister-pack, the samples were incubated at $36\pm 2\text{ }^{\circ}\text{C}$ for $18+4\text{ h}$.

Vegetative cells and spores of *Clostridium perfringens* were enumerated using membrane filtration and an internal validation method based on UNE-EN ISO 7937 (2005) [31] and UNE-EN 26461-2 (1995) [32]. Different sample volumes (100, 10, 1 and 0.1 mL) were filtered through a 0.22 μm -pore-size mixed cellulose ester membrane filter (Millipore, Molsheim, France). The filter was placed face up on tryptose sulfite cycloserine agar (Oxoid, Basingstoke, UK), with D-Cycloserine selective supplement and 4-methylumbelliferylphosphate (Merck, Darmstadt, Germany), and it was anaerobically incubated at $44\pm 1\text{ }^{\circ}\text{C}$ for $21\pm 3\text{ h}$ inside a jar with anaerobic gas generating sachets Genbox anaer (BioMérieux, Marcy l'Etoile, France) and an Anaerotest[™] anaerobic indicator strip (Merk, Darmstadt, Germany). To enumerate *C. perfringens*, plates were examined under long-wave UV light, and those presenting fluorescence were counted as positive results.

The detection and enumeration of intestinal enterococci were carried out using a membrane filtration method based on the ISO Standard 7899-2:2000 [33]. Serial dilutions of water samples (100, 10, 1 and 0.1 mL) were filtered through a 0.45 μm -pore-size mixed cellulose ester filter (Millipore, Darmstadt, Germany). The filter was placed on Slanetz and Bartley agar (Merck, Darmstadt, Germany) and incubated at $36\text{ }^{\circ}\text{C}\pm 2\text{ }^{\circ}\text{C}$ for $44\pm 4\text{ h}$. Colonies with red pigmentation were considered presumptive and were confirmed as

intestinal enterococci if they turned brown or black after incubation at 44 °C for 4 h on bile esculin azide agar (Merck, Darmstadt, Germany).

Somatic coliphages (SOMCPH) were concentrated and enumerated by a double-layer agar method adapted from ISO 10705-2:2000 [34] and ISO 10705-3:2003 [35,36]. Samples were processed by direct inoculation or membrane filtration depending on the matrix. For RW samples, 0.1 mL and 1 mL were analyzed by direct inoculation. For the first group of samples (pretreatment stages), membrane filtration of 500–1000 mL was needed, whereas for the second group (GW and treatment stages), volumes ranging from 6 to 10 mL were processed by direct inoculation, as they corresponded to eluates concentrated by Rexeed.

2.4. Physicochemical and Climatological Data

A range of physicochemical data was measured *in situ* during sampling: sample temperature (°C), conductivity ($\mu\text{S}/\text{cm}$), turbidity (NTU), pH, ammonium ($\text{mg NH}_4^+/\text{L}$), total organic carbon (TOC: $\text{mg C}/\text{L}$), percentages of RW and GW intake, river flow rate (m^3/s) and residual amounts of the disinfectants chlorine dioxide, ozone and chlorine (ppm).

Climatological data were also recorded in the Sant Joan Despí DWTP meteorological station and retrieved from the Meteorological Service of Catalonia, including temperature (°C), relative humidity (%) and rainfall ($\text{mm}/24\text{ h}$).

2.5. Metabarcoding by 16S rRNA Gene Amplicon Sequencing

To characterize bacterial diversity in the water ecosystem, metabarcoding was performed by paired-end amplicon sequencing. Two-run metabarcoding was applied to a total of 104 samples: 72 DWTP samples, 2 event samples, 8 additional samples used to check reproducibility between the different runs, 16 whole-procedure blanks (from each sampling to sequencing), 4 negative controls (from PCR to sequencing), and 2 positive controls (ZymoBIOMICS™ microbial community DNA standard (mock community) (Zymo research, Irvine, CA, USA)). A total of 6 DWTP samples were removed from the dataset, as they presented low reads and were sequenced in a third run.

2.5.1. PCR Amplification of DNA

The 16S rRNA V4 genomic region was amplified by PCR using barcoded primers 515F and 806R [37]. A detailed list containing the sequences of primers, sample barcodes and leading Ns can be found in Table S1. For all samples (5–10 ng total DNA), PCR was performed using 10 μL of AmpliTaq gold 360 Master Mix (Applied Biosystems, Bedford, MA, USA), 0.16 μL of bovine serum albumin, 1.84 or 5.84 μL of nuclease-free water, 2 μL of primer mix (4 μL of each 5 μM forward and reverse primer and 72 μL water) and 2 or 6 μL of sample-extracted DNA in a total volume of 20 μL per sample. PCR cycling conditions followed the protocol of Caporaso [37]. Briefly, the reaction started with a denaturation procedure held at 95 °C for 3 min. Then, 35 amplification cycles were set at 94 °C for 45 s, 50 °C for 60 s and 72 °C for 90 s. A final extension of 10 min at 72 °C was added. All samples were run with negative and positive controls of PCR blanks and mock communities, respectively. The PCR products were checked by visualization on 1% agarose gel containing purple 6x loading dye and by a reference 1 Kb DNA extension ladder marker (Invitrogen, Waltham, MA, USA).

2.5.2. Amplicon Multiplexing, Library Preparation and Illumina Sequencing

Multiplexing of samples was performed by pooling 10 μL of each barcoded amplicon. Library preparation consisted of PCR amplicon clean-up by the MinElute PCR Purification Kit (Qiagen, Hilden, Germany), and DNA quantification consisted of purified PCR products by the Qubit dsDNA BR Assay Kit (Invitrogen, Waltham, MA, USA). The DNA PCR-free protocol was used to prepare a multiplexed paired-end library for Illumina sequencing by the NEXTflex PCR-Free DNA Sequencing Kit (Bioo Scientific, Austin, TX, USA). The library was quantified by qPCR using the NEBNext Library Quant Kit (Illumina, San Diego, CA, USA), and the NEBioCalculator web tool was used for qPCR NGS library quantification

(<https://nebiocalculator.neb.com/>, accessed on 26 July 2019) to achieve optimal cluster densities and therefore an optimal sequence output. Multiplexed libraries with barcoded samples were spiked with 1% bacteriophage PhiX genome (PhiXControl Library; Illumina, San Diego, CA, USA) and were sequenced by the Illumina MiSeq platform using the 600-cycle 2×300 bp paired-end sequencing MiSeq Reagent Kit v3 (Illumina, San Diego, CA, USA) with a loading concentration of 20 pM.

2.5.3. Bioinformatic Analyses

The resulting FASTQ files were checked for quality (>90% of bases with a Phred quality score >Q30), processed and analyzed using Cutadapt [38], DADA 2 [39], QIIME2 [40] and Phyloseq [41] pipelines. Cutadapt was used to demultiplex samples (assign sequences to their sample) and to trim adapters, primers, barcodes and leading Ns from sequencing reads. A DADA 2 workflow was performed to denoise the sequences.

Firstly, quality filtering and the trimming of sequences was set to 200 bp (for forward reads) and 190 bp (for reverse reads) with a maximum number of expected errors allowed per read set at 1 (EE = 1). Then, samples with zero reads and low-quality sequences were deleted. Filtered sequences were dereplicated, the forward and reverse reads were aligned and merged, chimeras were removed and an amplicon sequence variant (ASV) table was obtained. Taxonomy was assigned to the resulting sequence variants with a pre-trained Naive Bayes classifier [42] using the SILVA SSU 138 reference database and was imported to the phyloseq R package for microbiome analyses.

To obtain more accurate profiling of microbial communities, the decontam R package [43] was used to remove sequences derived from contaminating DNA present in extraction or sequencing reagents that may interfere with samples.

2.6. Data Analyses

Statistical analyses were performed using the statistical software R version 4.0.5 (<https://www.r-project.org>, accessed on November 2021). For water quality, data were $\log_{10}(x + 1)$ transformed, and the Kruskal–Wallis test was used to assess differences in culturable and molecular parameters throughout the DWTP.

The phyloseq package [41] was used to analyze and visualize sequencing data.

Biodiversity was evaluated by analyzing the relative abundance of reads with the vegan package. Chao1 and Shannon indices were used to study alpha diversity. Beta diversity was also explored, representing sample groups (treatment stages) in a non-metric multidimensional scaling (NMDS) matrix by Bray–Curtis dissimilarities. Temperature impact was measured with both alpha (Pearson correlation) and beta diversity (PERMANOVA analysis). SIMPER analyses were also performed by the vegan package to identify which amplicon sequence variants contributed most to the differences between the DWTP stages. SourceTracker2 [44] was used to estimate the influence of the water source and treatment stages on the bacterial communities downstream.

3. Results

3.1. Sample Collection, and Physicochemical and Climatological Data

Climatological data as well as basic DWTP operating conditions are summarized in Table S2. Temperatures ranged from 11.5 to 29.5 °C, and humidity ranged from 44 to 71%. Episodes of rainfall 24 h before sampling were reported in 2 out of 8 samplings (N1 and N8), but the amounts were small (0.4 and 2.9 mm, respectively). When moderate or heavy rainfall occurred, sampling was postponed to avoid large weather-induced differences between samples. River flow rate ranged between 5.39 and 135 m³/s.

Some operational data were also measured: the percentage of RW or GW intake and the percentage of water processed by conventional or advanced treatments (Table S2). In 2 out of 8 samplings, RW accounted for almost 100% of water intake for the treatment procedure, whereas both RW and GW were used for the rest of the sampling.

Physicochemical data recorded for samples are synthesized in Table S3. Regarding temperature, RW was more variable than GW, averaging at 15 °C (5.6–23.4 °C). In contrast, GW presented a more stable temperature throughout the sampling campaign, with an average of 18 °C (16.1–20.2 °C). The average temperature of the final drinking water was 18 °C (8.5–25.3 °C).

3.2. Culturable Water Quality Indicators

The quality of all water samples taken from the DWTP was examined by determining culturable fecal indicators, as shown in Figure 2. The data obtained follow a non-normal distribution, and the water quality varied at each sampling point. The Kruskal–Wallis test was significant for each culturable indicator at all DWTP stages ($p < 0.00001$).

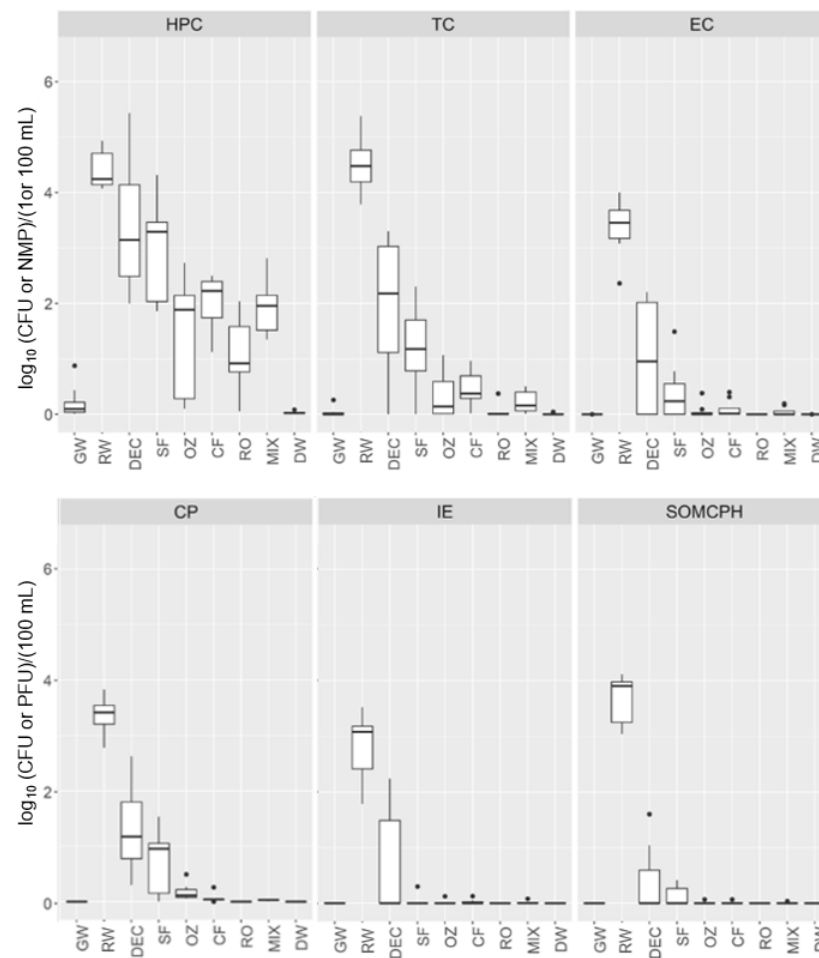


Figure 2. Boxplot of microbial analysis of water samples collected at different treatment stages in the DWTP: heterotrophic plate counts (HPC, CFU/mL), total coliforms (TC, NMP/100 mL), *E. coli* (EC, NMP/100 mL), *Clostridium perfringens* (CP, CFU/100 mL), intestinal enterococci (IE, CFU/100 mL) and somatic coliphages (SOMCPH, PFU/100 mL). Samples represented: groundwater (GW), river water (RW), decantation (DEC), sand filtration (SF), ozonization (OZ), carbon filtration (CF), reverse osmosis (RO), mixing chamber (MIX) and post-chlorination water (DW).

RW samples had the highest concentration of bacterial indicators (average CFU/100 mL or NMP/100 mL: 3 \log_{10} intestinal enterococci (IE), 3.5 \log_{10} *Clostridium perfringens* (CP), 3.6 \log_{10} *E. coli* (EC) and 4.7 \log_{10} total coliforms (TC)), as well as the highest concentration of viral indicator somatic coliphages (SOMCPH; average 3.8 \log_{10} PFU/100 mL) and HPC (average 4.5 \log_{10} CFU/mL), whereas for GW, all water quality parameters were negative except for the HPC, with very few colonies (<7 CFU/mL) observed in some samples.

The dynamics of microbial indicators varied throughout DWTP processing. Samples from the pretreatment stages had a high HPC, especially at DEC (average $4.58 \log_{10}$ CFU/mL), being similar to those of the RW intake. After the SF stage, the HPC was reduced by an average of 1 log with respect to the DEC stage. Subsequently, a 2 and 3 log reduction in HPC was observed after the conventional and advanced treatments, respectively.

In addition, DEC and SF samples presented a 2 and 3 log reduction in TC, EC and CP, a 1.5 and 4 log reduction in IE and a 3 and 4 log reduction in SOMCPH, respectively. However, although TC decreased after DEC and SF and were further reduced by CF, their complete removal required RO. Thus, TC reduction was 4 log by conventional treatment and 5 log by advanced processing. The same trends were observed for the other indicators (EC, CP and IE), with 4 log reductions achieved by conventional treatment and 5 to 6 log removal by advanced treatment.

In the MIX samples, the HPC was similar to that of CF ($\sim 2 \log_{10}$ CFU/mL); TC levels were very low, ranging from 0.03 to 2.2 NMP/100 mL; and IE was detected in one sample (0.2 CFU/100 mL).

The DEUF method revealed the presence of microbial indicators below the detection limit of the standard ISO methods (< 1 CFU/100 mL), thereby allowing a more accurate determination of the efficiency of the different treatments. Thus, positive results for *C. perfringens* were obtained until CF, whereas TC, EC, IE and SOMCPH were detected further downstream until the MIX, with negative results in the post-chlorination water. All microbial indicators after chlorination were below the limits established by European drinking water regulations, with the HPC revealing no or very few colonies (< 0.2 CFU/mL).

3.3. Metabarcoding

An overview of the metabarcoding results according to sequencing depth and diversity at all treatment stages is shown in Table 1.

Table 1. Overview of the 16S DWTP sample dataset showing the number of raw reads, filtered reads, total amplicon sequence variants (ASVs), number of core ASVs and mean and standard deviation values (mean \pm sd) of alpha diversity for richness (Chao1) and diversity (Shannon).

Sampling		Metabarcoding				α -Diversity	
DWTP Stages	No. Samples	Raw Reads (Input)	Filtered Reads (Output)	Total ASVs	Core ASVs	Richness (Chao1)	Diversity (Shannon)
GW	8	1,658,112	831,634	2320	43	731 \pm 143	5.17 \pm 0.18
RW	8	1,891,711	1,048,230	1873	48	525 \pm 241	4.65 \pm 0.76
DEC	8	1,793,904	1,060,600	2244	3	448 \pm 182	4.07 \pm 0.46
SF	8	2,206,287	1,321,279	2359	31	561 \pm 242	4.19 \pm 0.50
OZ	8	1,646,557	953,977	1942	4	378 \pm 133	3.66 \pm 0.51
CF	8	2,212,847	1,335,303	2416	81	691 \pm 258	4.87 \pm 0.67
RO	8	1,501,907	920,979	1736	31	432 \pm 169	4.32 \pm 0.42
MIX	8	1,694,781	1,045,001	2146	51	583 \pm 282	4.80 \pm 0.75
DW	8	2,325,282	1,478,535	1417	20	314 \pm 108	3.34 \pm 0.68
Total	72	16,931,388	9,995,538	10,039			

After carrying out quality filtering, the 16S dataset of all DWTP samples comprised a total of 9,995,538 reads with an average of $\sim 138,826$ reads per sample (ranging from 40,959 to 274,999 reads). Negative controls ranged from 1627 to 6627 reads. Overall, the number of ASVs obtained by denoising was 10,039.

3.4. Diversity Analysis

The microbial diversity of the 72 water samples was investigated by ASV analysis. After rarefaction at the minimum number of reads obtained in the dataset (40,959), alpha and beta diversity were studied. The rarefaction curves show that all samples reached a plateau, suggesting good representation of bacterial communities (Figure S1).

3.4.1. Alpha Diversity Patterns

Species richness and diversity were examined by analyzing the average relative abundances of ASVs using the species richness estimate (Chao1) and the Shannon diversity index for each sample (Table 1 and Figure 3). Different trends in richness and diversity were observed according to the processing stage of the DWTP.

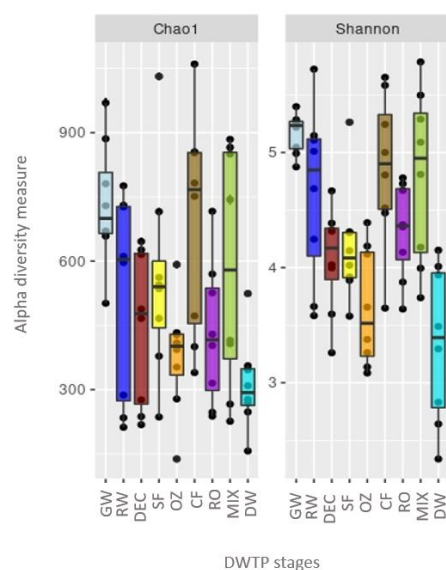


Figure 3. Boxplots representing alpha diversity indices of ASV richness (Chao1) and diversity (Shannon) for all DWTP samples: groundwater (GW), river water (RW), decantation (DEC), sand filtration (SF), ozonization (OZ), carbon filtration (CF), reverse osmosis (RO), mixing chamber (MIX) and post-chlorination water (DW).

The Chao index was higher for GW (731) than for RW (525). In pretreatment, a decrease in richness was observed at DEC (448), followed by a slight increase after SF (561). During the conventional treatment, a decrease was observed after OZ (378), followed by a huge increase after the subsequent CF (691), which produced the second highest richness value overall. In the advanced treatment, RO led to a considerable reduction in richness, producing the third lowest value (432). In the mixing chamber, richness increased again (583), only to be significantly reduced by the final chlorination (314). Thus, the lowest number of ASVs were obtained after OZ and in the final drinking water, whereas the highest number of reads corresponding to different ASVs within samples were found in GW, in CF and in the MIX.

Shannon indices reveal high diversity in all DWTP samples, with the values ranging from 3.3 to 5.2, showing a similar trend to that of the Chao index, with only minor differences at certain stages. Although diversity was slightly higher in GW (5.17) than in RW (4.65), the difference is not statistically significant ($p = 0.67$). After DEC (4.07), diversity values significantly reduced ($p < 0.01$) and remained the same after SF (4.19). In the conventional treatment, OZ led to a small reduction in diversity (3.66), which then increased significantly ($p < 0.01$) after CF (4.87). Similar values were obtained between RO (4.32) and SF samples as well as between MIX (4.8) and CF samples. Regarding species richness, chlorination drastically reduced diversity (3.34, $p = 0.0001$). Thus, the lowest diversity values, indicating a more uniform species composition, were obtained after OZ and in the

final drinking water, whereas the GW samples, followed by CF and MIX samples, had the highest values.

Alpha diversity was also analyzed by the Kendal correlation between the relative abundance of each ASV, and no significant correlation was found.

3.4.2. Beta Diversity Patterns

To explore differences in the bacterial community between different steps of the potabilization process, non-metric multidimensional scaling (NMDS) plots were constructed using the Bray–Curtis coefficient of sequencing results. Samples are represented, and ellipses indicate standard deviation of within-sample variance (Figure 4). All the eight samplings corresponding to the same matrices cluster together, although with a certain dispersion. GW and RW intakes are clearly separated along the second axis, and both are also separated from DW along the first and second axis. One of the GW samples (N4) is separate from the others, corresponding to a period when the DWTP was operating with 100% RW (as shown in Table 1).

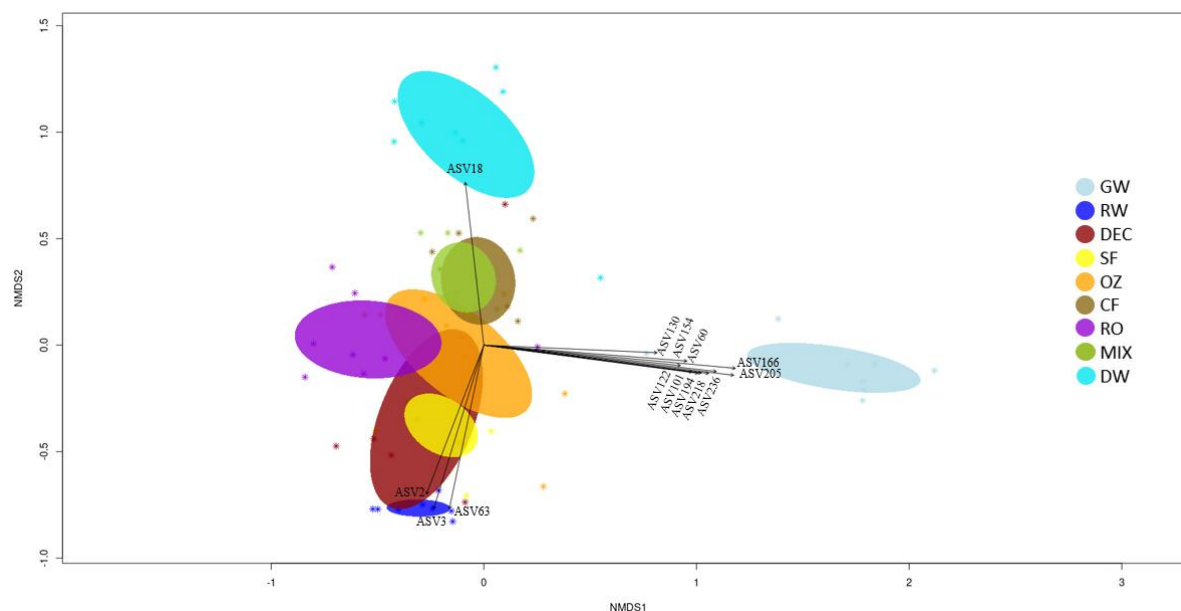


Figure 4. Bray–Curtis dissimilarity matrix (non-metric multidimensional scaling (NMDS)) of the 72 DWTP samples color-coded according to each sample type: groundwater (GW), river water (RW), decantation (DEC), sand filtration (SF), ozonization (OZ), carbon filtration (CF), reverse osmosis (RO), mixing chamber (MIX) and post-chlorination water (DW). Ellipses represent standard deviations of samples. The ten most abundant ASVs ($p = 0.001$) of samples from each treatment are illustrated with vectors that describe more precisely the differences within DWTP samples along both axes. GW (greyish blue) and DW (turquoise) show the least similarity with other sample types.

A partial overlap between ellipses appears for pretreatment stages and for conventional (OZ, CF) and advanced treatments (RO), and an overlap can be observed between SF and DEC samples and between FC and MIX samples.

The ten most abundant ASVs ($p < 0.001$) in DWTP samples at each treatment stage were vectorized into the Bray–Curtis nMDS representation (Figure 4). Samples of GW, RW and DW are clearly separated from these stages.

Significant vectors that separate GW samples along the first axis correspond to Planctomycetota [ASV60 (Candidatus Brocardia), ASV130 and ASV154 (GWA2-50-13 family)], Patescibacteria [ASV218 (UBA9983 order) and ASV236 (Candidatus Giovannonibacteria order)], Verrucomicrobiota [ASV101, ASV122 and ASV194 (Candidatus Omnitrophus)] and unclassified others [ASV166 (unclassified bacteria) and ASV205 (unclassified Myxococota)]. Along the second axis, it can be seen that ASV18 was influential for the chlorinated

samples (DW), and ASV2, ASV3 and ASV63 best describe RW intake. RW was mainly represented by Proteobacteria (unclassified Comamonadaceae family and *Limnohabitans*), and Bacteroidota (*Flavobacterium*), whereas Cyanobacteria (*Candidatus Obscuribacter*) particularly defined the chlorinated samples.

3.4.3. Bacterial Communities at Each Treatment Stage

The samples from water sources and treatments presented variable taxonomic profiles, although some consistencies in taxa were observed throughout the DWTP. The taxonomy results at the DWTP based on the relative abundance of reads on a phylum and class level are shown in Figure 5.

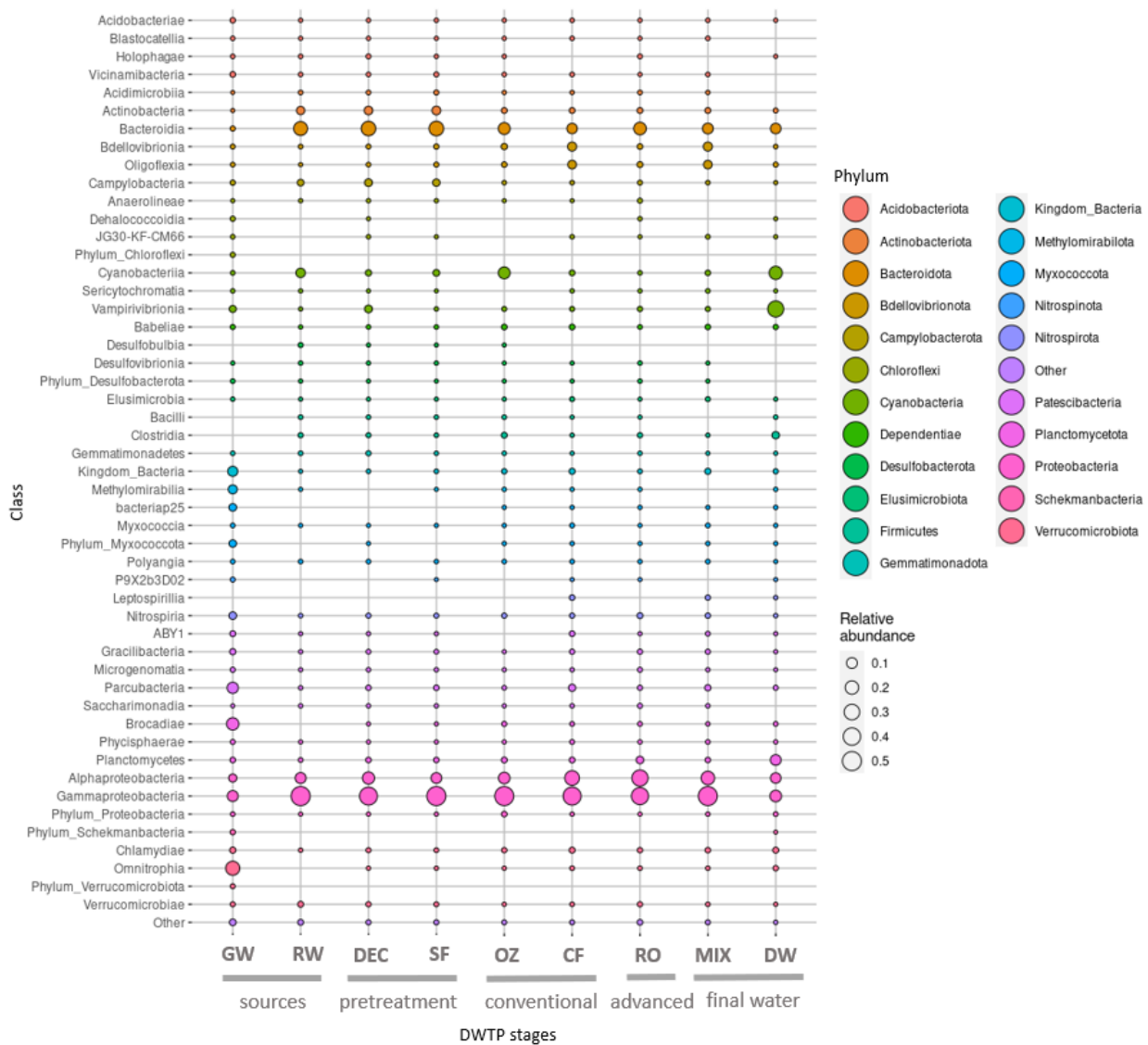


Figure 5. Bubble plot diagram showing the relative abundance (%) of ASVs grouped according to class for each DWTP stage: groundwater (GW), river water (RW), decantation (DEC), sand filtration (SF), ozonation (OZ), carbon filtration (CF), reverse osmosis (RO), mixing chamber (MIX) and post-chlorination water (DW). Bubble size indicates the relative abundance of each bacterial class. On the right, each class is grouped in the corresponding superior taxonomic classification (phyla).

The most abundant phylum throughout the DWTP was Proteobacteria (ranging from 57% to 73%), except in the final post-chlorination drinking water (21%). Bacteroidota

(0.8–27%) and Bdellovibrionota (1–12%) were the second and third most abundant phyla at all stages.

Among Proteobacteria, the class Gammaproteobacteria predominated throughout the DWTP, and Alphaproteobacteria increased after DEC, CF, RO and the MIX. Bacteroidia was the second most dominant class in RW and pretreatment samples, undergoing a reduction downstream.

The most abundant Proteobacteria genus corresponded to *Limnohabitans*.

For a more detailed taxonomy for all samples at different hierarchy levels, see the Krona diagrams in Figure S2.

The top 50 ASVs correspond to approximately 41% of the total microbial composition in all the DWTP samples and belong to a total of 33 genera.

Taxonomy profiles of the two different water sources differed considerably in terms of phyla. Although the GW community showed higher phyla variability, ASVs were mainly affiliated to Verrucomicrobiota (25%), Planctomycetota (17%), Patescibacteria (15%) and Proteobacteria (14%). These were followed by unclassified bacteria (8%) and Methyloirabilota (5%), among others, and Candidatus Omnitrophus (23%) was the most abundant genus. In RW, Proteobacteria predominated (63%), followed by Bacteroidota (21%), Cyanobacteria (6%) and Actinobacteriota (5%), and the most abundant genera were *Limnohabitans* (12%) and *Flavobacterium* (11%) (Figure 6).

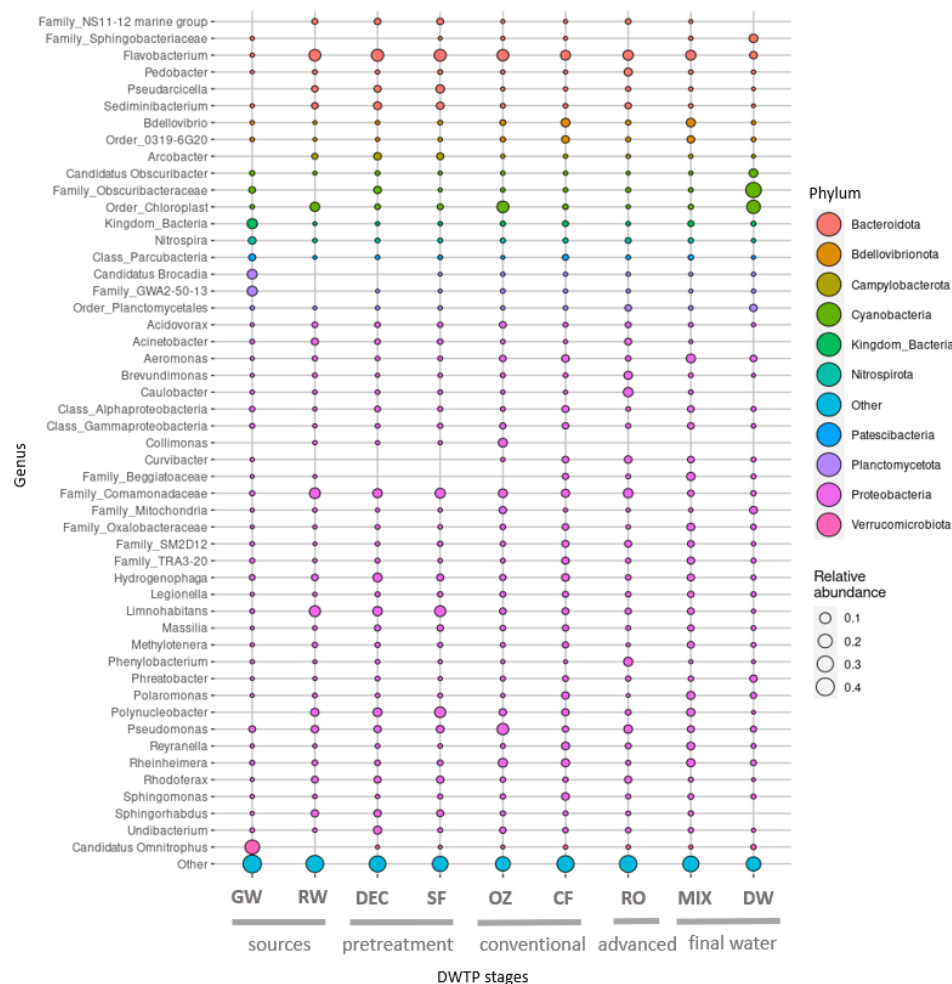


Figure 6. Bubble plot diagram showing the relative abundance (%) of ASVs grouped at the genus level for each DWTP stage: groundwater (GW), river water (RW), decantation (DEC), sand filtration (SF), ozonization (OZ), carbon filtration (CF), reverse osmosis (RO), mixing chamber (MIX) and post-chlorination water (DW). Bubble size indicates the relative abundance of each bacterial genus. On the right side, each class is grouped into their corresponding superior taxonomic classification (phyla).

In pretreatment, profiles of phylum, class and genus were similar between DEC and SF samples, and the most abundant genera were *Limnohabitans* (7% and 10%, respectively) and *Flavobacterium* (14% and 15%, respectively). These genera were also dominant in RW.

In the conventional treatment, the first significant shift in bacterial distribution was observed after OZ, which resulted in a clear increase in Cyanobacteria (19%) and a slight decrease in Bacteroidota (11%), and the community remained dominated by Proteobacteria (63%). A reduction in Campylobacteriota (0.09%) and Actinobacteriota (0.8%) was also apparent. The most abundant genera were *Flavobacterium* (9%), *Collimonas* (8%) and *Pseudomonas* (8%), although a higher number of reads were affiliated to an unclassified Chloroplast order (18%). In the following CF step, Proteobacteria and Bacteroidota remained largely unchanged. However, Cyanobacteria (1%) abundance was lower, and Bdellovibrionota (11%) was higher. The reads corresponded, above all, to Proteobacteria (70%), Bdellovibrionota (10%) and Bacteroidota (9%). The genera *Flavobacterium* (7%), *Bdellovibrio* (5%), *Rheinheimera* (4%), *Aeromonas* (3%) and *Pseudomonas* (2%) were the most abundant.

After RO, the proportion of Proteobacteria (73%) was higher compared to SF and GW samples, whereas Bacteroidota abundance (16%) was higher than in GW but lower than in SF. Abundance of Patescibacteria (1%), Plactomycetota (3%) and Verrucomicrobiota (1%) was lower than in GW but was similar to SF samples. *Flavobacterium* (8%), *Caulobacter* (7%), unculturable Comamonadaceae (7%) and *Pseudomonas* (5%) were the most common genera found.

In the MIX, where the conventional and advanced treatments converge, the taxonomy patterns were very similar to CF samples, with Proteobacteria (69%), Bacteroidota (12%) and Bdellovibrionota (12%) predominating. The most abundant genera were *Flavobacterium* (7%) and *Bdellovibrio* (6%), and *Legionella* was also found (2%).

Finally, the biggest shift in bacterial composition was observed in DW, where the predominant phylum was Cyanobacteria (56%). Notable proportions of Proteobacteria (21%) and Bacteroidota (8%) were also found, but the former was much less abundant than in the MIX. Firmicutes (3%) increased 100-fold, whereas the dominant genera belonged to the family Obscuribacteraceae (31%) and an unclassified Chloroplast order (20%).

3.5. Core Bacterial Communities at the DWTP

Taxa shared across the different samples were identified to determine the core communities in the DWTP and at each treatment stage. Although no ASVs were shared among all samples at all sampling sites, different core ASVs were found at each treatment stage, as shown in Table 1. Very few core ASVs were detected in samples of DEC and OZ (3 out of 2244 and 4 out of 1942, respectively), corresponding to the genera *Limnohabitans*, *Porphyrobacter* and *Sediminibacterium* in DEC samples and *Aeromonas*, *Polynucleobacter*, *Porphyrobacter* and *Sphingorhabdus* in OZ samples.

Conversely, when samples were clustered according to ambient temperature (low ≤ 18 °C and high ≥ 22 °C), differences in core communities were observed. The samples from the pretreatment steps until the MIX had very few ASVs in common: ASV2 (*Limnohabitans*) and ASV161 (*Reyranella*) at low temperatures and only ASV 16 (*Aeromonas*) at high temperatures. On the other hand, samples had more core ASVs at high than at low temperatures, except for GW and DEC. Venn diagrams showing the number of unique core ASVs and shared ASVs between high and low temperatures are provided in Figure 7.

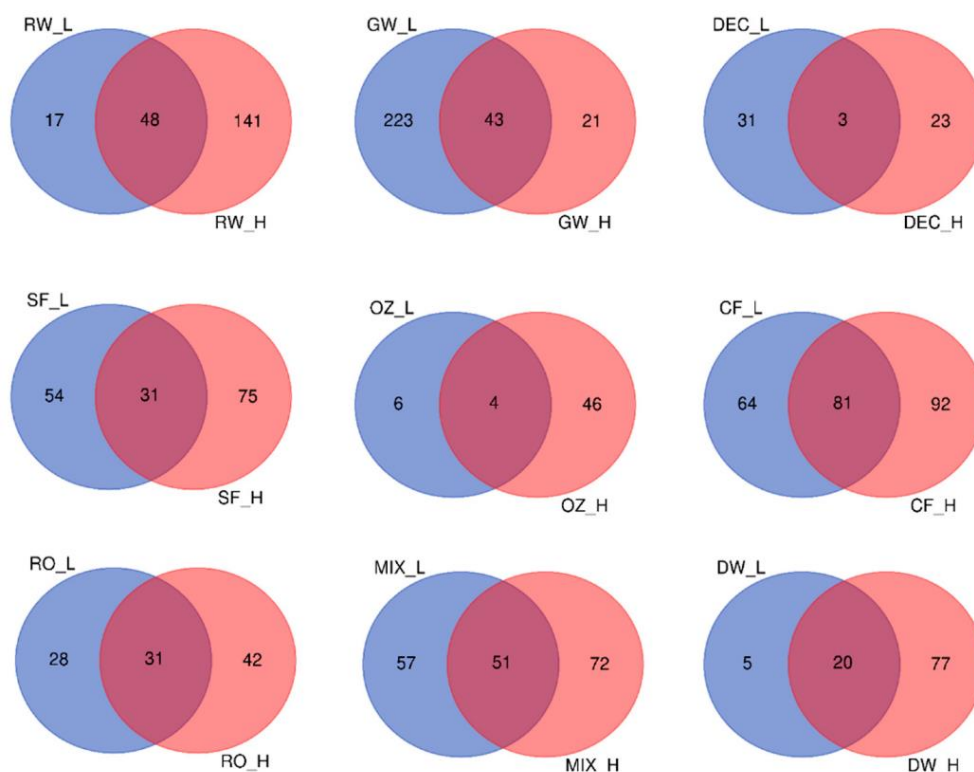


Figure 7. Venn diagrams showing the total number of shared or unique core ASVs for each treatment stage: groundwater (GW), river water (RW), decantation (DEC), sand filtration (SF), ozonization (OZ), carbon filtration (CF), reverse osmosis (RO), mixing chamber (MIX) and post-chlorination water (DW). Samples are separated by low (L, in blue) or high (H, in red) temperatures.

3.6. Impact of Temperature on Bacterial Communities

A moderate positive correlation between alpha diversity (Shannon index) and ambient temperature was found for some of the treatment stages, including DEC ($r = 0.73$) and CF ($r = 0.83$). A lower correlation was also found at other stages, but their values are not significant (RW $r = 0.57$, SF $r = -0.30$; OZ $r = 0.37$, RO $r = 0.51$, MIX $r = 0.31$, DW $r = 0.31$).

Beta diversity correlation with temperature was examined by permutational multivariate analysis of variance (PERMANOVA) of rarefied ASVs based on a Bray–Curtis dissimilarity matrix (Table S4). PERMANOVA analysis gave significant results for the temperature factor.

Regarding taxonomy profiles at high (HT) and low temperatures (LT) (Figure S3), differences in bacterial composition were found in some stages.

The bacterial composition in GW remained quite similar. In contrast, a moderate (non-significant) correlation with temperature was observed in RW, where Proteobacteria was always dominant (~70%). However, Bacteroidota was more abundant at LT (28%) than at HT (19%), and Actinobacteriota abundance was 10-fold greater at HT (8%) than at LT (0.8%). The main genera at LT were *Flavobacterium* (24%), *Limnohabitans* (22%) and unknown Comamonadaceae (14%). The abundance of the latter remained unchanged when temperatures increased, but a reduction was observed in *Flavobacterium* (7%).

Temperature was responsible for a significant shift in DEC samples; at LT, Bacteroidota was the major phylum (51%), followed by Proteobacteria (34%) and Campylobacterota (14%), whereas at HT, Proteobacteria dominated (84%), Bacteroidota abundance decreased (15%), and no reads of Campylobacterota were obtained. The predominant genus at LT was *Flavobacterium* (41%), and at HT, it was *Limnohabitans* (35%).

Although the composition in SF samples remained generally similar, Actinobacteriota was only detected at HT (9%), and the genus *Pseudomonas* (7%) was only detected at

LT. Moreover, *Flavobacterium* was more prevalent at LT (25%) than at HT (6%), when *Polynucleobacter* became predominant (20%).

At the OZ stage, temperature strongly affected bacterial composition; at LT, the major phyla were Proteobacteria (58%) and Cyanobacteria (42%), and at HT, Proteobacteria remained predominant (66%). However, Cyanobacteria reads were negligible (0.08%), being displaced by Bacteroidota (33%), which was not detected at LT. The most abundant genera at LT were *Pseudomonas* (46%) and unclassified genera from the Chloroplast order (42%), neither of which were observed at HT, when most reads were for *Flavobacterium* (33%) and *Rheinheimera* (19%).

Bacterial composition in CF samples was also significantly correlated with the season, with diversity increasing with temperature. Proteobacteria (83%) reads clearly dominated at LT and were lower at HT (71%), when Bacteroidota abundance increased (12%). *Flavobacterium* (10%) remained unchanged, whereas *Polynucleobacter* (10%) was detected only at HT, and *Sphingomonas* (8%) was only detected at LT.

The correlation with temperature at the RO stage was moderate (non-significant), with a clear dominance of Proteobacteria (94%) at HT. The reads decreased at LT (65%), when the next most abundant phylum was Bacteroidota (34%), which was scarcely detected at HT (0.4%). The most abundant genera at LT were *Flavobacterium* (19%) and *Pseudomonas* (13%), and at HT, they were *Caulobacter* (21%) and *Phenylobacterium* (18%).

In the MIX samples, temperature-associated differences at the genus and superior taxa level were statistically insignificant. Although the reads for *Flavobacterium* remained constant (~10%), *Polynucleobacter* (15%) was only detected at HT, followed by *Aeromonas* (14%), and at LT, *Polaromonas* (11%) was second in abundance.

In the final DW, a moderate but non-significant correlation with temperature was observed, with an obvious dominance of Cyanobacteria (87%) at LT, which was reduced somewhat at HT (63%) when Planctomycetota (12%) and Firmicutes (8%) were also detected. However, their levels were otherwise very low at LT (0.6% and 0.4%, respectively). The dominant genus in DW at LT was an unknown member of the Obscuribacteraceae family (58%), which was less abundant at HT (27%) when it accounted for half of the reads jointly, with unclassified reads belonging to the Chloroplast order (27%). The proportions of *Clostridium sensu stricto 1* (6%) and *Aeromonas* (5%) were greater at HT than at LT (0.4% and 0%, respectively). Regarding the ASV distribution according to temperature, the 50 most abundant core ASVs at HT and LT throughout the DWTP are illustrated in Figure 8.

3.7. Tracking the Origin of the ASVs along the DWTP

To investigate which upstream stages in the DWTP contribute most to the microbial communities downstream, samples corresponding to the final stages were analyzed by the SourceTracker algorithm. Intake water, pretreatment stages, as well as conventional and advanced treatments were treated as “source”, whereas the final stages, the MIX and post-chlorination drinking water (DW) were “sink” samples. The results of the analysis are shown in Table 2. Before the chlorination stage (Table 2), the reads from the MIX samples mainly matched those of CF (89.7%), with some also corresponding to SF (2.7%), RO (2%) and unknown sources (4.4%). However, after the chlorination stage (Table 2), most of the reads from the DW were from unknown sources (67.9%), followed by the OZ stage (17.4%) and the MIX (7.9%). GW and RO also contributed to the bacterial communities of the final chlorinated water (1.4% and 2%, respectively), whereas the contribution of CF was negligible (0.2%), despite being the main source of reads at the MIX stage.

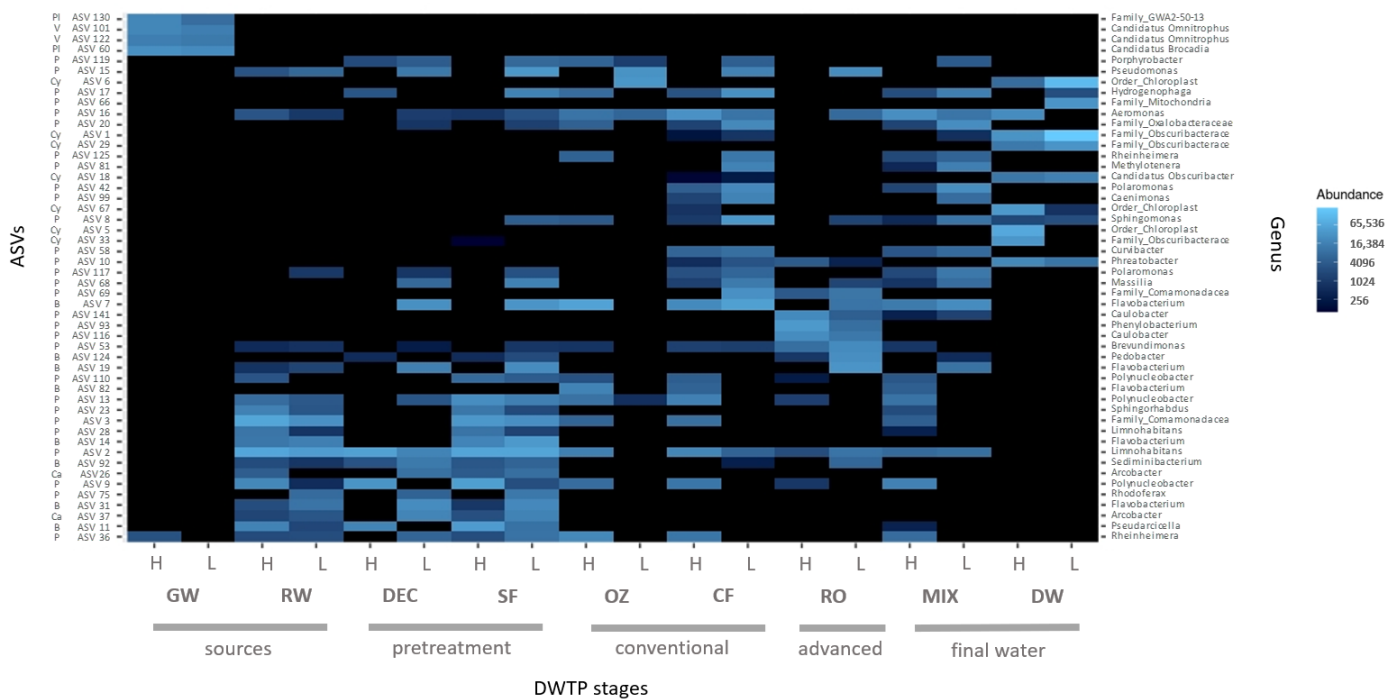


Figure 8. Heatmap of read abundances of the top 50 most abundant core ASVs in 72 DWTP samples: groundwater (GW), river water (RW), decantation (DEC), sand filtration (SF), ozonization (OZ), carbon filtration (CF), reverse osmosis (RO), mixing chamber (MIX) and post-chlorination water (DW). Samples are grouped according to the temperature of the sampling campaign, being either high (H) or low (L). Data are illustrated by a gradient color scale from black (not detected) to light blue (high relative abundance). On the left, the phyla classification for each ASV is indicated by one of the following codes: Bacteroidota (B), Campylobacterota (Ca), Cyanobacteria (Cy), Proteobacteria (P), Planctomycetota (Pl) or Verrucomicrobiota (V). ASV classification at the genus level is shown on the right.

Table 2. Average contribution of each source (DWTP stages) to bacterial communities in the MIX sink and DW sink. Samples correspond to: groundwater (GW), river water (RW), decantation (DEC), sand filtration (SF), ozonization (OZ), carbon filtration (CF), reverse osmosis (RO), mixing chamber (MIX) and post-chlorination water (DW).

	GW	RW	DEC	SF	OZ	CF	RO	MIX	Unknown
Mean (MIX used as sink)	0.0%	0.2%	0.1%	2.7%	0.9%	89.7%	2.0%	-	4.4%
SD	0.0%	0.2%	0.2%	4.7%	1.3%	5.2%	2.5%	-	4.0%
Mean (DW used as sink)	1.4%	0.0%	0.1%	0.0%	17.4%	0.2%	2.0%	7.9%	67.9%
SD	3.9%	0.0%	0.2%	0.0%	25.2%	0.2%	5.5%	22.2%	39.9%

3.8. Surface Water Contamination Episode and Changes in Operational Procedures

Water quality values of GW and CF samples during the river contamination event were similar to those registered in the other sampling campaigns; in GW, all bacterial indicators were negative, whereas only 5 NMP/100 mL for TC and 1 NMP/100 mL for EC were detected in CF samples. HPC accounted for 0.48 CFU/mL and 104 CFU/mL in GW and CF, respectively.

The taxonomic profile in GW during the event was similar to that of the other GW samples, with no evident changes in water quality parameters and metabarcoding results. However, metabarcoding analysis revealed different diversity patterns in the CF water

in comparison with the samples taken under usual operating conditions (Figure S4). Although the phyla remained the same, there were some differences in relative abundance of Proteobacteria (30% lower), Bdellovibrionota, (22% lower), and Verrucomicrobiota (7.6% higher). Differences were also observed in ASV composition: 126 ASVs were shared with core CF samples (at low temperatures), and a total of 711 unique ASVs were found in CF samples during the event. At the genus level, *Bdellovibrio* was dominant (18%), followed by unclassified members of the Oligoflexia order 0319-6G20 (7%), *Reyranella* (7%) and Candidatus Omnitrophus (6%), whereas CF samples taken at low temperatures contained *Flavobacterium* (10%), *Sphingomonas* (8%), *Hydrogenophaga* (7%) and *Polaromonas* (6%), among others. Nonetheless, these results should be interpreted with caution, as only one sample was studied, and it may reflect occasional operational variation in the carbon filters.

The suspension of RW intake allowed us to track the effect of GW on CF communities, as none of the other pretreatment stages were in operation. As seen in Figure 9, CF effectively removed Acidobacteriota and Methylomirabilota from the GW and reduced Myxococcota, Patescibacteria, Planctomycetota and Verrucomicrobiota. However, an increase in Bdellovibrionota (from 0.2% to 26%) and Proteobacteria (from 4% to 53%) was observed in the CF samples.

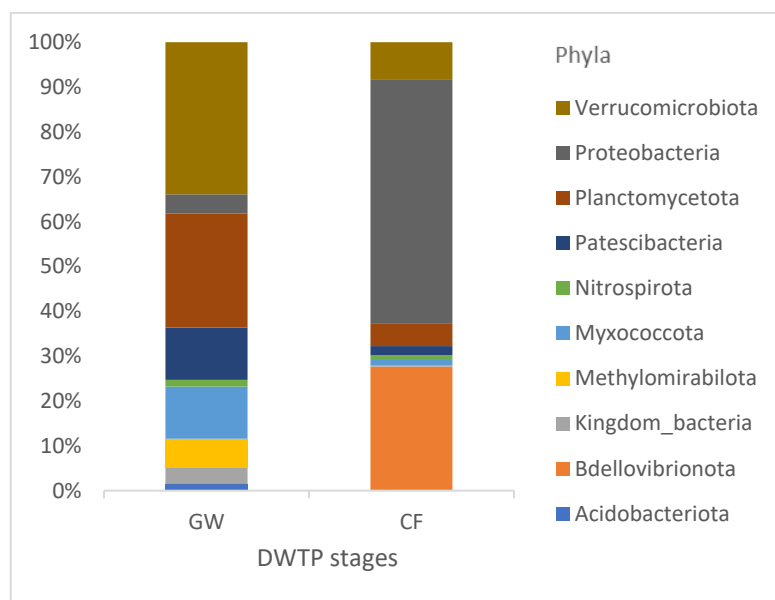


Figure 9. Bar charts of ASV relative abundance, indicating phyla in groundwater (GW) and carbon filtration (CF) samples during the river contamination episode.

3.9. Detection of Microbial Indicators and Potential Pathogens by 16SrRNA Sequencing

Sequences of bacterial groups relevant for water systems based on the Global Water Pathogens list [45] were found. A total of eight potentially pathogenic bacterial genera were identified in the DWTP with a very low relative abundance of reads (0.002 to 8%) (Table S5). *Pseudomonas* was detected at the OZ stage (8%) and in the DW (1%), *Aeromonas* and *Legionella* were detected in the MIX (4% and 2%, respectively) and DW (2% and 0.4%, respectively) and *Clostridium* was detected in OZ (1%) and DW (2%). Other potentially pathogenic genera, *Arcobacter*, *Campylobacteriales*, *Escherichia-Shigella* and *Mycobacterium*, were only detected in source water or at early treatment stages, with their abundance being very low (<1%) in later treatments or in the final DW. *Helicobacter*, *Leptospira* and *Vibrio* were not detected in any sample.

Regarding data on culturable water quality indicators (Section 3.2.), it was observed that culturable *E. coli*, an indicator of fecal contamination, accounted for an average of 3.5 log₁₀ CFU/100 mL in RW, whereas in metabarcoding analysis, it contributed only 0.003% of reads for *Escherichia-Shigella*. Additionally, *Clostridium sensu stricto* 1 was

found in DW in low abundance (2%), although it was higher than in the previous stages (0.002–0.02%), but no culturable *C. perfringens* was detected in the DW. Finally, *Enterococcus* was only detected in very low abundance (0.002%) in SF, OZ and CF.

4. Discussion

The performance of an advanced full-scale DWTP was assessed using culturable microbial indicators, as indicated in the current EU Directive on drinking water together with molecular methods (16S rRNA metabarcoding). Monitoring the dynamics of bacterial communities in a DWTP may help to better understand process performance, allowing a more in-depth assessment of operational variations that may modify water quality. For example, nutrient excess in source water may lead to regrowth of microorganisms or biofilm formation [3,46], which can affect the taste and odor of tap water and may even result in an increase in opportunistic pathogens, posing a risk to public health. Moreover, an increase in cyanobacterial blooms in surface water may produce clogging in filtration stages as well as being a health hazard, as some genera are toxin producers [2].

Although the quality of the analyzed drinking water complies with EU Directive regulations, the stipulated culture-based indicators were not able to detect changes in bacterial communities in the DWTP. For example, the HPC remained constant despite shifts in bacterial diversity.

The use of a DEUF concentration method allowed the reduction in microbial indicators to be monitored more precisely during water processing, especially in the advanced treatment stages, when indicator concentration is very low and not detected by conventional techniques. Thus, among the culturable indicators, *C. perfringens* was traced until carbon filtration, and total coliforms, *E. coli*, intestinal enterococci and somatic coliphages were detected until the mixing chamber, with no traces remaining in the final drinking water. Historical data from this DWTP (from 2011 to 2019, data not shown), based on the use of standard membrane filtration for routine water quality monitoring, indicate positive results for these indicators only at early stages (i.e., *E. coli* and somatic coliphages until sand filtration, or intestinal enterococci until carbon filtration). Previous studies using the DEUF method have reported recoveries of 45.5 ± 24.0 % for fecal indicators and 22.4 ± 9.3 % for bacteriophages [47], ranging from 35 to 95% for enteric bacteria and viruses [48] or 60–80% for bacteria, viruses and protozoa in drinking water [20], depending on the water matrix and degree of turbidity. Therefore, the reported concentrations for the different indicators may be even higher than in the current study.

Compared to other methods, DEUF allowed for more in-depth and representative characterization of the bacterial communities in the DWTP, as large water volumes could be sampled. Contaminants from DNA extraction kits or PCR reagents can confound the results of molecular analysis, especially in samples with a low microbial biomass, such as the final treated water [49]. In this context, large volume concentration methods are particularly useful. In our PCR procedure, sequence blanks clustered together, indicating that they did not significantly interfere with the characterization of the DWTP microbiome.

High diversity was observed at all DWTP stages, being the highest in GW, followed by the MIX and CF samples. Overall species abundance and richness were significantly reduced by the treatments, especially disinfection, with the lowest values being obtained in the OZ, DW and DEC samples. River water, the main intake source of the DWTP, had a lower species richness than those of the SF, FC and MIX samples. The higher diversity observed at SF and CF may indicate an established microbiome associated with filtration procedures, as has been reported [13]. Diversity at the DEC stage was lower than it was after the following step of SF, reflecting a loss in richness after the disinfection procedure with chlorine dioxide and possible bacterial regrowth in the filters. A similar trend was observed in the conventional treatment, with a decrease in diversity after OZ, followed by a high increase in CF samples and again with a decrease in the advanced treatment, where there was reduced species richness at the RO stage. Diversity in the mixing chamber was high, falling between the values of the CF and SF samples. Finally, chlorination significantly

reduced species diversity in the final water. Chlorine has a strong bactericidal effect, damaging bacterial cell structure, although certain groups resist the disinfection process. ASVs of bacterial communities characterized at disinfection stages may correspond to chlorine-resistant strains of *Aeromonas*, *Clostridium*, Cyanobacteria or *Pseudomonas*, among others (reviewed in Luo et al. [50]). Low diversity in RO samples can be explained by the low nutrient levels in permeate water, where only specially adapted microorganisms can thrive. Genera detected at this stage include *Caulobacter*, *Comamonas*, *Curvibacter*, *Flavobacterium* and *Pseudomonas*, which are considered potentially biofilm-forming.

Although Bdellovibrionota was detected at different treatment stages with $\leq 1\%$ abundance, it accounted for 10 and 12% of reads in the CF and MIX samples, respectively, mainly consisting of unculturable Oligoflexia and *Bdellovibrio*. The members of this phylum are described as obligate predators of bacteria (Gram-negative and Gram-positive) and have been proposed as biocontrol agents for their ability to prey on multi-drug-resistant bacteria [51]. Concerning core amplicon sequence variants, only one ASV was detected in the samples taken at high temperatures and two in the samples taken at low temperatures, which correspond to *Aeromonas* and to *Limnohabitans* and *Reyranella*, respectively. The detection of core ASVs under the standard operational conditions of the DWTP is of interest, as they can provide new monitoring tools for detecting impaired treatments, a potential application that still needs more research.

Over the short period when GW was the only source of intake and when the routine operational conditions of the DWTP changed, an increase in certain bacterial populations at the CF stage was detected, which can be attributed to the growth of communities present in biofilms in the filter or to their temporal detachment from carbon surfaces. Such conditions can be met after a sudden shift of water intake for the exclusive use of GW and can be attributed to differences in temperatures compared with other water sources [52]. In this study, in the winter season when this episode occurred, river water temperature gathered at 7.9 °C, whereas groundwater presented 17.1 °C on the day of sampling. Nevertheless, in the current study, the significance of these results may be limited by the unrepresentativeness of the samples. Different potabilization stages exerted a selective pressure on bacterial communities and shaped their composition downstream. Filtration procedures had a strong influence, which is in agreement with other studies on sand filtration [13] and carbon filtration [16,53]. However, disinfection had a greater impact, as reported previously, as residual disinfectants reduce the abundance and diversity of bacterial communities, which become dominated by resistant genera (including opportunistic pathogens) in post-chlorination water [14,15,54] and in distribution networks [54–56]. In the present study, the chlorination stage shifted the dominant bacterial population in the final drinking water from Proteobacteria to Cyanobacteria, a phylum that was poorly represented in source water (0–3%) and at other treatment stages (<6%), being slightly higher in OZ samples (19%). The aphotic environment of many of these processes (but not the pretreatment) suggests that the unclassified Cyanobacteria that were detected are non-photosynthetic. The dominant genus in the DW belongs to the unculturable Obscuribacteraceae, which are found in dark conditions, followed by an unclassified Chloroplast order. Most databases, such as SILVA, classify chloroplasts within the Cyanobacteria phylum, as they are considered a phylogenetic lineage evolved from endosymbiotic Cyanobacteria [57]. Thus, chloroplast reads are commonly found in aquatic environments, and have been reported in studies of river [58] and lake [59] water quality.

Little is known about the diversity and ecology of non-photosynthetic Cyanobacteria in water environments, and their classification is still under debate. Di Rienzi and colleagues [60] proposed their inclusion in a sibling phylum, Melainabacteria (named after “Melaina”, a nymph of dark waters in Greek mythology), whose sequenced genomes confirm an absence of a photosynthetic apparatus. Another study suggests that the orders Obscuribacterales and Vampirovibrionales, which are capable of aerobic and anaerobic respiration, should also be included in this new phylum [61]. Although the SILVA database does not phylogenetically differentiate the non-photosynthetic cyanobacterial

group, Cyanobacteria have been reported in aphotic environments, such as groundwater and animal guts [60], koala feces and activated sludge from a wastewater treatment plant [61] and continental subsurfaces 420–607 m in depth [62].

Although most studies characterizing bacterial communities in DWTP stages and drinking water have not detected Cyanobacteria and report Proteobacteria as the dominant phylum [11,13–15,25,55,63,64], other researchers have obtained a high abundance of Cyanobacteria reads in water from distribution networks [8], treatment stages [65] or sludge storage in drinking water processing [65,66]. These variable results may be accounted for by factors such as location, the type and quality of source water, and whether or not disinfectant procedures are used, all of which create a unique habitat in each DWTP or distribution network. Cyanobacteria cells have an outer peptidoglycan layer thicker than most Gram-negative bacteria and a cell wall mainly composed of lipids and carotenoids. Furthermore, the outer membrane has fewer conductance porins than most Gram-negative bacteria, which is an adaptation to low-nutrient environments that enhances resistance toward harmful chemicals [57]. This structure may confer mechanical stability when exposed to chlorine, with chlorine-resistant groups being found in the final water. No cyanobacterial blooms, stagnation or microcystin (cyanobacterial toxins) were detected in the river or drinking water, which was safe for consumption.

Changes in microbial communities related to ambient temperature were also observed in different treatment stages, with a correlation of higher diversity with higher temperatures, specially at DEC and CF. Such temporal variability has been widely described [10,13,14,67]. Higher temperatures can trigger changes in bacterial communities, as they facilitate bacterial growth of different genera. Implications of high temperatures in water systems have been documented, such as the occurrence of certain waterborne bacterial pathogens, opportunistic pathogens and biofilm-forming groups that may compromise water quality or pose a risk to public health. For instance, Calero Preciado et al. (2021) [3] observed a significant increase in relative abundant reads of *Pseudomonas* and *Fusarium* in chlorinated distribution networks favored by temperature, both with the capability to promote biofilm formation. Moreover, the presence of the opportunistic pathogen *Mycobacterium* spp. was also registered to rise together with temperature. Other genera that promote biofilm development in chlorinated distribution networks, such as *Aeromonas*, also show greater abundance at higher temperatures [68]. Similarly, in unchlorinated drinking water supplies, van der Wielen and van der Kooij (2013) [69] described a higher occurrence of *Legionella pneumophila* and *Stenotrophomonas maltophilia* at high temperatures. Both of them are likely to grow in biofilms and can be moderately to highly virulent, as they often cause pneumonia or bacteremia disease, respectively, in immunocompromised patients. These observed changes related to temperature may be of interest to drinking water managers in the context of the global warming scenario.

Very few 16S rRNA sequences (0.002–8%) retrieved from the source water and treatment stages were associated with genera of waterborne bacterial pathogens in the global priority list. Reads of *Aeromonas*, *Arcobacter*, the order Campylobacterales, *Legionella*, *Mycobacterium*, *Escherichia-Shigella* and *Pseudomonas* detected in the DWTP were reduced or eliminated in the DW, except for *Pseudomonas* and *Aeromonas* (1% and 2%). *Arcobacter* reads, which were low in RW and pretreatment stages (1–3%), were negligible in drinking water (0.007%), demonstrating the effectiveness of conventional and advanced treatments in removing *Arcobacter* species, as previously shown by Collado et al. (2010) [70]. *Helicobacter*, *Leptospira* and *Vibrio* were not detected at any stage of the process. It should be mentioned that not all the species of the targeted potentially pathogenic genera are animal, human or plant pathogens. Additionally, the reads may correspond to non-viable or dead cells after the potabilization treatment or to free DNA. The present analysis of drinking water samples confirms that the applied potabilization process provides safe drinking water, free of fecal indicators.

Discrepancies were observed in the results between conventional culture-based techniques and metabarcoding. In RW, culturable *E. coli* values were high (3.5 log₁₀ CFU/100 mL),

but the abundance of reads was very low (0.003%), perhaps because of a PCR bias against rare taxa in non-treated water samples. In DW, the opposite occurred with *C. perfringens*, which was detected by the molecular technique (3%) but not by culture. However, relative abundance data must be treated with caution, as high-throughput sequencing is not designed for quantitative purposes. Therefore, the analysis of water quality based only on sequencing methods can lead to inaccurate assessments of microbial hazards [54]. Nevertheless, a molecular approach allows for the simultaneous tracking of pathogens, opportunistic pathogens, microbial indicators and their fluctuations between treatments and within samples. The resulting taxonomic data can be used to develop quantitative methods such as qPCR to provide a more comprehensive understanding of microbial population dynamics.

Both approaches to water quality monitoring (culture- and molecular-based) have benefits and limitations. Although microbial indicators and HPC offer protection against pathogens and can detect viable microorganisms, the results can be biased by the medium or by growth conditions, and changes in microbial composition are not detected. In this respect, 16S rRNA metabarcoding provides a more in-depth analysis of microbial communities, including both culturable and non-culturable, autotrophic and heterotrophic, photic and aphotic and waterborne bacteria. However, metabarcoding also has shortcomings: obtaining results is more time-consuming; there is no standardized methodology; rare taxa can be neglected due to primer bias; and cell viability remains unconfirmed, which hinders risk assessment [71]. Although all drinking water samples in this study fully met the quality standards of the EU Directive, samples with a stable HPC were observed to have variable bacterial diversity. Therefore, the use of 16S rRNA metabarcoding in water quality management in combination with standardized techniques can provide useful information on the efficiency of the different stages of water treatment and may help to address the challenge of potabilization related to likely expected deterioration of surface water due to future climate threats that may compromise water quality.

5. Conclusions

The application of 16S rRNA metabarcoding to assess microbial communities in a full-scale DWTP in Barcelona (Spain), which uses two different water sources, a pretreatment stage and a combination of conventional and advanced treatments with final chlorination, provides new insights into compositional changes throughout the process.

Highly diverse microbial communities were observed, suggesting that each treatment stage has specific microbiota, including unculturable bacteria.

Differences in community structure can be explained by the water sources, the type of treatment applied at each stage (especially filtration and chlorination procedures), microhabitats or biofilm formation in carbon filtration and, to a lesser extent, seasonal variations in ambient temperature. Proteobacteria was the dominant phylum in source water and throughout the procedure, with a big shift after the chlorination stage when it was displaced by Cyanobacteria, which was previously found in low abundance, except at the ozonization stage.

The studied drinking water met all the quality standards stipulated by the EU Directive. However, molecular analysis revealed that bacterial diversity, even in samples with a stable HPC, differs throughout the process. Therefore, the use of 16S rRNA metabarcoding in combination with standardized parameters provides a more in-depth analysis of the microbiota in a DWTP, which can be useful for the detection of operational variations and for their impact on water quality.

Supplementary Materials: The following supporting information can be downloaded at: <https://www.mdpi.com/article/10.3390/w14091435/s1>. Supplementary material associated with this article: Supplementary File S1 (Tables S1–S5 and Figure S1). Supplementary File S2 (interactive version of Figure S2): Figure S2. Krona plots of the relative abundance reads of bacteria detected by 16S metabarcoding at all DWTP stages: groundwater (GW), river water (RW), decantation (DEC), sand filtration (SF), ozonization (OZ), carbon filtration (CF), reverse osmosis (RO), mixing chamber (MIX) and post-chlorination drinking water (DW). Taxonomic profiles are simultaneously displayed

by hierarchy levels from kingdom to genus by selecting taxonomic depths: 1: Kingdom 2: Phylum 3: Class 4: Order 5: Family 6: Genus. Supplementary File S3 (interactive version of Figure S3): Figure S3. Krona charts of the core community bacteria detected by 16S metabarcoding at all DWTP stages grouped by sampling time at high (H) or low temperatures (L): groundwater (GW), river water (RW), decantation (DEC), sand filtration (SF), ozonization (OZ), carbon filtration (CF), reverse osmosis (RO), mixing chamber (MIX) and post-chlorination drinking water (DW). Taxonomic profiles are simultaneously displayed by hierarchy levels from kingdom to genus by selecting taxonomic depths: 1: Kingdom 2: Phylum 3: Class 4: Order 5: Family 6: Genus. Supplementary File S4 (interactive version of Figure S4): Figure S4. Krona charts of relative abundant core ASVs in groundwater (GW_core_L) and CF (FC_core_L) taken at low temperatures under usual operating conditions, and GW (GW_Cont_Episode) and CF (CF_Cont_Episode) during the river contamination episode.

Author Contributions: A.P.-M. performed sampling and water quality analysis; A.P.-M. and O.S.W. carried out the metabarcoding experiments; A.P.-M., O.S.W., J.M. and C.G.-A. processed the data analysis; C.G.-A., A.R.B., B.G., K.P. and O.S.W. conceived and supervised the study; A.P.-M. wrote the manuscript. All authors contributed intellectual content and revised the manuscript. All authors have read and agreed to the published version of the manuscript.

Funding: This research was funded by Pla de Doctorats Industrials of the Catalan Government grant number 2016 DI 083.

Institutional Review Board Statement: Not applicable.

Informed Consent Statement: Not applicable.

Data Availability Statement: The original DNA sequences are available upon request.

Acknowledgments: This study was supported by Pla de Doctorats Industrials of the Catalan Government (2016 DI 083) and the Water Research Institute. We thank Jordi Martin, Marta Ganzer and Sergio Montes for their support and expertise in DWTP procedures. The graphical abstract and Figure 1 were created with BioRender.com, accessed on 15 February 2022.

Conflicts of Interest: The authors declare no conflict of interest.

References

1. Whitehead, P.G.; Wilby, R.L.; Battarbee, R.W.; Kernan, M.; Wade, A.J. A review of the potential impacts of climate change on surface water quality. *Hydrol. Sci. J.* **2009**, *54*, 101–123. [[CrossRef](#)]
2. O'Neil, J.M.; Davis, T.W.; Burford, M.A.; Gobler, C.J. The rise of harmful cyanobacteria blooms: The potential roles of eutrophication and climate change. *Harmful Algae* **2012**, *14*, 313–334. [[CrossRef](#)]
3. Calero Preciado, C.; Boxall, J.; Soria-Carrasco, V.; Martínez, S.; Douterelo, I. Implications of Climate Change: How Does Increased Water Temperature Influence Biofilm and Water Quality of Chlorinated Drinking Water Distribution Systems? *Front. Microbiol.* **2021**, *12*, 658927. [[CrossRef](#)] [[PubMed](#)]
4. Li, W.; Zhang, J.; Wang, F.; Qian, L.; Zhou, Y.; Qi, W.; Chen, J. Effect of disinfectant residual on the interaction between bacterial growth and assimilable organic carbon in a drinking water distribution system. *Chemosphere* **2018**, *202*, 586–597. [[CrossRef](#)]
5. Favere, J.; Barbosa, R.G.; Sleutels, T.; Verstraete, W.; De Gussem, B.; Boon, N. Safeguarding the microbial water quality from source to tap. *NPJ Clean Water* **2021**, *4*, 28. [[CrossRef](#)]
6. Prest, E.I.; Hammes, F.; van Loosdrecht, M.C.M.; Vrouwenvelder, J.S. Biological stability of drinking water: Controlling factors, methods, and challenges. *Front. Microbiol.* **2016**, *7*, 45. [[CrossRef](#)]
7. Prest, E.I.; El-Chakhtoura, J.; Hammes, F.; Saikaly, P.E.; van Loosdrecht, M.C.M.; Vrouwenvelder, J.S. Combining flow cytometry and 16S rRNA gene pyrosequencing: A promising approach for drinking water monitoring and characterization. *Water Res.* **2014**, *63*, 179–189. [[CrossRef](#)]
8. Liu, T.; Kong, W.; Chen, N.; Zhu, J.; Wang, J.; He, X.; Jin, Y. Bacterial characterization of Beijing drinking water by flow cytometry and MiSeq sequencing of the 16S rRNA gene. *Ecol. Evol.* **2016**, *6*, 923–934. [[CrossRef](#)]
9. Lautenschlager, K.; Hwang, C.; Liu, W.T.; Boon, N.; Köster, O.; Vrouwenvelder, H.; Egli, T.; Hammes, F. A microbiology-based multi-parametric approach towards assessing biological stability in drinking water distribution networks. *Water Res.* **2013**, *47*, 3015–3025. [[CrossRef](#)]
10. Romero, P.E.; Calla-Quispe, E.; Castillo-Vilcahuaman, C.; Yokoo, M.; Fuentes-Rivera, H.L.; Ramirez, J.L.; Ampuero, A.; Ibáñez, A.J.; Wong, P. From the Andes to the desert: 16S rRNA metabarcoding characterization of aquatic bacterial communities in the Rimac river, the main source of water for Lima, Peru. *PLoS ONE* **2021**, *16*, e0250401. [[CrossRef](#)]
11. Chao, Y.; Ma, L.; Yang, Y.; Ju, F.; Zhang, X.X.; Wu, W.M.; Zhang, T. Metagenomic analysis reveals significant changes of microbial compositions and protective functions during drinking water treatment. *Sci. Rep.* **2013**, *3*, 3550. [[CrossRef](#)]

12. Shaw, J.L.A.; Monis, P.; Weyrich, L.S.; Sawade, E.; Drikas, M.; Cooper, A.J. Using amplicon sequencing to characterize and monitor bacterial diversity in drinking water distribution systems. *Appl. Environ. Microbiol.* **2015**, *81*, 6463–6473. [[CrossRef](#)] [[PubMed](#)]
13. Pinto, A.J.; Xi, C.; Raskin, L. Bacterial Community Structure in the Drinking Water Microbiome Is Governed by Filtration Processes. *Environ. Sci. Technol.* **2012**, *46*, 8851–8859. [[CrossRef](#)]
14. Hou, L.; Zhou, Q.; Wu, Q.; Gu, Q.; Sun, M.; Zhang, J. Spatiotemporal changes in bacterial community and microbial activity in a full-scale drinking water treatment plant. *Sci. Total Environ.* **2018**, *625*, 449–459. [[CrossRef](#)] [[PubMed](#)]
15. Li, Q.; Yu, S.; Li, L.; Liu, G.; Gu, Z.; Liu, M.; Liu, Z.; Ye, Y.; Xia, Q.; Ren, L. Microbial Communities Shaped by Treatment Processes in a Drinking Water Treatment Plant and Their Contribution and Threat to Drinking Water Safety. *Front. Microbiol.* **2017**, *8*, 2465. [[CrossRef](#)] [[PubMed](#)]
16. Bruno, A.; Sandionigi, A.; Bernasconi, M.; Panio, A.; Labra, M.; Casiraghi, M. Changes in the drinking water microbiome: Effects of water treatments along the flow of two drinking water treatment plants in a urbanized area, milan (Italy). *Front. Microbiol.* **2018**, *9*, 2557. [[CrossRef](#)] [[PubMed](#)]
17. Belila, A.; El-Chakhtoura, J.; Otaibi, N.; Muyzer, G.; Gonzalez-Gil, G.; Saikaly, P.E.; van Loosdrecht, M.C.M.; Vrouwenvelder, J.S. Bacterial community structure and variation in a full-scale seawater desalination plant for drinking water production. *Water Res.* **2016**, *94*, 62–72. [[CrossRef](#)] [[PubMed](#)]
18. Rhodes, E.R.; Hamilton, D.W.; See, M.J.; Wymer, L. Evaluation of hollow-fiber ultrafiltration primary concentration of pathogens and secondary concentration of viruses from water. *J. Virol. Methods* **2011**, *176*, 38–45. [[CrossRef](#)] [[PubMed](#)]
19. Hill, V.R.; Kahler, A.M.; Jothikumar, N.; Johnson, T.B.; Hahn, D.; Cromeans, T.L. Multistate Evaluation of an Ultrafiltration-Based Procedure for Simultaneous Recovery of Enteric Microbes in 100-Liter Tap Water Samples. *Appl. Environ. Microbiol.* **2007**, *73*, 4218–4225. [[CrossRef](#)]
20. Gunnarsdottir, M.J.; Gardarsson, S.M.; Figueras, M.J.; Puigdomènech, C.; Juárez, R.; Saucedo, G.; Arnedo, M.J.; Santos, R.; Monteiro, S.; Avery, L.; et al. Water safety plan enhancements with improved drinking water quality detection techniques. *Sci. Total Environ.* **2020**, *698*, 134185. [[CrossRef](#)]
21. EPA; CDC. *Comparison of Ultrafiltration Techniques for Recovering Biothreat Agents in Water*; EPA/600/R-11/103; U.S. Environmental Protection Agency: Washington, DC, USA, 2011.
22. Ferrari, S.; Frosth, S.; Svensson, L.; Fernström, L.L.; Skarin, H.; Hansson, I. Detection of *Campylobacter* spp. in water by dead-end ultrafiltration and application at farm level. *J. Appl. Microbiol.* **2019**, *127*, 1270–1279. [[CrossRef](#)] [[PubMed](#)]
23. Cuevas-Ferrando, E.; Randazzo, W.; Pérez-Cataluña, A.; Sánchez, G. HEV Occurrence in Waste and Drinking Water Treatment Plants. *Front. Microbiol.* **2020**, *10*, 2937. [[CrossRef](#)] [[PubMed](#)]
24. Francy, D.S.; Stelzer, E.A.; Brady, A.M.G.; Huitger, C.; Bushon, R.N.; Ip, H.S.; Ware, M.W.; Villegas, E.N.; Gallardo, V.; Lindquist, H.D.A. Comparison of filters for concentrating microbial indicators and pathogens in lake water samples. *Appl. Environ. Microbiol.* **2013**, *79*, 1342–1352. [[CrossRef](#)]
25. Wang, F.; Li, W.; Li, Y.; Zhang, J.; Chen, J.; Zhang, W.; Wu, X. Molecular analysis of bacterial community in the tap water with different water ages of a drinking water distribution system. *Front. Environ. Sci. Eng.* **2018**, *12*. [[CrossRef](#)]
26. Revetta, R.P.; Pemberton, A.; Lamendella, R.; Iker, B.; Santo Domingo, J.W. Identification of bacterial populations in drinking water using 16S rRNA-based sequence analyses. *Water Res.* **2010**, *44*, 1353–1360. [[CrossRef](#)]
27. Martin-Alonso, J. Barcelona's water supply improvement: The brine collector of the Llobregat river. *Water Sci. Technol.* **1994**, *30*, 221–227. [[CrossRef](#)]
28. Directive (EU) 2020/2184 of the European Parliament and of the Council of 16 December 2020 on the Quality of Water Intended for Human Consumption. Available online: <https://eur-lex.europa.eu/legal-content/EN/LSU/?uri=CELEX:32020I284>. (accessed on 23 January 2022).
29. *International Standard ISO 6222:1999*; Water Quality—Enumeration of Culturable Micro-Organisms—Colony Count by Inoculation in a Nutrient Agar Culture Medium. International Organization for Standardization: Geneva, Switzerland, 1999.
30. *International Standard ISO 9308-2:2012*; International Standard Water Quality—Enumeration of *Escherichia coli* and Coliform bacteria—Part 2: Most Probable Number Method. International Organization for Standardization: Geneva, Switzerland, 2012.
31. *UNE-EN ISO 7937:2005*; Microbiology of Food and Animal Feeding Stuffs—Horizontal Method for the Enumeration of *Clostridium Perfringens*—Colony-Count Technique. International Organization for Standardization: Geneva, Switzerland, 2005.
32. *UNE-EN ISO 26461-2:1995*; Water Quality—Detection and Enumeration of the Spores of Sulfite-Reducing Anaerobes (Clostridia): Part 2: Method by Membrane Filtration. International Organization for Standardization: Geneva, Switzerland, 1995.
33. *International Standard ISO 7899-2:2000*; Water Quality—Detection and Enumeration of Intestinal Enterococci—Part 2: Membrane Filtration Method. International Organization for Standardization: Geneva, Switzerland, 2000.
34. *International Standard ISO 10705-2:2000*; Water Quality—Detection and Enumeration of Bacteriophages—Part 2: Enumeration of Somatic Coliphages. International Organization for Standardization: Geneva, Switzerland, 2000.
35. Méndez, J.; Audicana, A.; Isern, A.; Llana, J.; Moreno, B.; Tarancón, M.L.; Jofre, J.; Lucena, F. Standardised evaluation of the performance of a simple membrane filtration-elution method to concentrate bacteriophages from drinking water. *J. Virol. Methods* **2004**, *117*, 19–25. [[CrossRef](#)]
36. *International Standard ISO 10705-3:2003*; Water Quality—Detection and Enumeration of Bacteriophages—Part 3: Validation of Methods for Concentration of Bacteriophages from Water. International Organization for Standardization: Geneva, Switzerland, 2003.

37. Caporaso, J.G.; Lauber, C.L.; Walters, W.A.; Berg-Lyons, D.; Lozupone, C.A.; Turnbaugh, P.J.; Fierer, N.; Knight, R. Global patterns of 16S rRNA diversity at a depth of millions of sequences per sample. *Proc. Natl. Acad. Sci. USA* **2011**, *108*, 4516–4522. [[CrossRef](#)]
38. Martin, M. Cutadapt removes adapter sequences from high-throughput sequencing reads. *EMB J.* **2011**, *17*, 10. [[CrossRef](#)]
39. Callahan, B.J.; McMurdie, P.J.; Rosen, M.J.; Han, A.W.; Johnson, A.J.A.; Holmes, S.P. DADA2: High resolution sample inference from Illumina amplicon data. *Nat. Methods* **2016**, *13*, 581–583. [[CrossRef](#)]
40. Bolyen, E.; Rideout, J.R.; Dillon, M.R.; Bokulich, N.A.; Abnet, C.C.; Al-Ghalith, G.A.; Alexander, H.; Alm, E.J.; Arumugam, M.; Asnicar, F.; et al. Reproducible, interactive, scalable and extensible microbiome data science using QIIME 2. *Nat. Biotechnol.* **2019**, *37*, 852–857. [[CrossRef](#)] [[PubMed](#)]
41. McMurdie, P.J.; Holmes, S. Phyloseq: An R Package for Reproducible Interactive Analysis and Graphics of Microbiome Census Data. *PLoS ONE* **2013**, *8*, e61217. [[CrossRef](#)] [[PubMed](#)]
42. Bokulich, N.A.; Kaehler, B.D.; Rideout, J.R.; Dillon, M.; Bolyen, E.; Knight, R.; Huttley, G.A.; Gregory Caporaso, J. Optimizing taxonomic classification of marker-gene amplicon sequences with QIIME 2's q2-feature-classifier plugin. *Microbiome* **2018**, *6*, 90. [[CrossRef](#)] [[PubMed](#)]
43. Davis, N.M.; Proctor, D.M.; Holmes, S.P.; Relman, D.A.; Callahan, B.J. Simple statistical identification and removal of contaminant sequences in marker-gene and metagenomics data. *Microbiome* **2018**, *226*. [[CrossRef](#)] [[PubMed](#)]
44. Knights, D.; Kuczynski, J.; Charlson, E.S.; Zaneveld, J.; Mozer, M.C.; Collman, R.G.; Bushman, F.D.; Knight, R.; Kelley, S.T. Bayesian community-wide culture-independent microbial source tracking. *Nat. Methods* **2011**, *8*, 761–763. [[CrossRef](#)]
45. Pruden, A.; Ashbolt, N.; Miller, J. Overview of issues for water bacterial pathogens. In *Water and Sanitation for the 21st Century: Health and Microbiological Aspects of Excreta and Wastewater Management*; Rose, J.B., Jiménez-Cisneros, B., Eds.; Global Water Pathogen Project; Part 3: Specific Excreted Pathogens: Environmental and Epidemiology Aspects—Section 2: Bacteria; Michigan State University: East Lansing, MI, USA; UNESCO: New York, NY, USA. [[CrossRef](#)]
46. Husband, S.; Fish, K.E.; Douterelo, I.; Boxall, J. Linking discoloration modelling and biofilm behaviour within drinking water distribution systems. *Water Sci. Technol. Water Supply* **2016**, *16*, 942–950. [[CrossRef](#)]
47. Pascual-Benito, M.; Emiliano, P.; Casas-Mangas, R.; Dacal-Rodríguez, C.; Gracenea, M.; Araujo, R.; Valero, F.; García-Aljaro, C.; Lucena, F. Assessment of dead-end ultrafiltration for the detection and quantification of microbial indicators and pathogens in the drinking water treatment processes. *Int. J. Hyg. Environ. Health* **2020**, *230*. [[CrossRef](#)]
48. Kahler, A.; Johnson, T.; Hahn, D.; Narayanan, J.; Derado, G.; Hill, V. Evaluation of an Ultrafiltration-Based Procedure for Simultaneous Recovery of Diverse Microbes in Source Waters. *Water* **2015**, *7*, 1202–1216. [[CrossRef](#)]
49. Salter, S.J.; Cox, M.J.; Turek, E.M.; Calus, S.T.; Cookson, W.O.; Moffatt, M.F.; Turner, P.; Parkhill, J.; Loman, N.J.; Walker, A.W. Reagent and laboratory contamination can critically impact sequence-based microbiome analyses. *BMC Biol.* **2014**, *12*, 87. [[CrossRef](#)]
50. Luo, L.W.; Wu, Y.H.; Yu, T.; Wang, Y.H.; Chen, G.Q.; Tong, X.; Bai, Y.; Xu, C.; Wang, H.B.; Ikuno, N.; et al. Evaluating method and potential risks of chlorine-resistant bacteria (CRB): A review. *Water Res.* **2021**, *188*, 116474. [[CrossRef](#)]
51. Kadouri, D.E.; To, K.; Shanks, R.M.Q.; Doi, Y. Predatory bacteria: A potential ally against multidrug-resistant Gram-negative pathogens. *PLoS ONE* **2013**, *8*. [[CrossRef](#)] [[PubMed](#)]
52. Moona, N.; Wünsch, U.J.; Bondelind, M.; Bergstedt, O.; Sapmaz, T.; Pettersson, T.J.R.; Murphy, K.R. Temperature-dependent mechanisms of DOM removal by biological activated carbon filters. *Environ. Sci. Water Res. Technol.* **2019**, *5*, 2232–2241. [[CrossRef](#)]
53. Oh, S.; Hammes, F.; Liu, W.T. Metagenomic characterization of biofilter microbial communities in a full-scale drinking water treatment plant. *Water Res.* **2017**, *128*, 278–285. [[CrossRef](#)] [[PubMed](#)]
54. Acharya, K.; Halla, F.F.; Massawa, S.M.; Mgana, S.M.; Komar, T.; Davenport, R.J.; Werner, D. Chlorination effects on DNA based characterization of water microbiomes and implications for the interpretation of data from disinfected systems. *J. Environ. Manag.* **2020**, *276*, 111319. [[CrossRef](#)]
55. Atnafu, B.; Desta, A.; Assefa, F. Microbial Community Structure and Diversity in Drinking Water Supply, Distribution Systems as well as Household Point of Use Sites in Addis Ababa City, Ethiopia. *Microb. Ecol.* **2021**. [[CrossRef](#)]
56. Bertelli, C.; Courtois, S.; Rosikiewicz, M.; Piriou, P.; Aeby, S.; Robert, S.; Loret, J.F.; Greub, G. Reduced chlorine in drinking water distribution systems impacts bacterial biodiversity in biofilms. *Front. Microbiol.* **2018**, *9*, 2520. [[CrossRef](#)]
57. Hoiczky, E.; Hansel, A. Cyanobacterial Cell Walls: News from an Unusual Prokaryotic Envelope. *J. Bacteriol.* **2000**, *182*, 1191–1199. [[CrossRef](#)]
58. Beale, D.J.; Karpe, A.V.; Ahmed, W.; Cook, S.; Morrison, P.D.; Staley, C.; Sadowsky, M.J.; Palombo, E.A. A community multi-omics approach towards the assessment of surface water quality in an urban river system. *Int. J. Environ. Res. Public Health* **2017**, *14*. [[CrossRef](#)]
59. Zhu, B.; Cao, H.; Li, G.; Du, W.; Xu, G.; Domingo, J.S.; Gu, H.; Xu, N.; Duan, S.; Lu, J. Biodiversity and dynamics of cyanobacterial communities during blooms in temperate lake (Harsha Lake, Ohio, USA). *Harmful Algae* **2019**, *82*, 9–18. [[CrossRef](#)]
60. Di Rienzi, S.C.; Sharon, I.; Wrighton, K.C.; Koren, O.; Hug, L.A.; Thomas, B.C.; Goodrich, J.K.; Bell, J.T.; Spector, T.D.; Banfield, J.F.; et al. The human gut and groundwater harbor non-photosynthetic bacteria belonging to a new candidate phylum sibling to Cyanobacteria. *eLife* **2013**, *2*, e01102. [[CrossRef](#)]
61. Soo, R.M.; Skennerton, C.T.; Sekiguchi, Y.; Imelfort, M.; Paech, S.J.; Dennis, P.G.; Steen, J.A.; Parks, D.H.; Tyson, G.W.; Hugenholtz, P. An expanded genomic representation of the phylum Cyanobacteria. *Genome Biol. Evol.* **2014**, *6*, 1031–1045. [[CrossRef](#)] [[PubMed](#)]

62. Puente-Sánchez, F.; Arce-Rodríguez, A.; Oggerin, M.; García-Villadangos, M.; Moreno-Paz, M.; Blanco, Y.; Rodríguez, N.; Bird, L.; Lincoln, S.A.; Tornos, F.; et al. Viable cyanobacteria in the deep continental subsurface. *Proc. Natl. Acad. Sci. USA* **2018**, *115*, 10702–10707. [[CrossRef](#)] [[PubMed](#)]
63. Sala-Comorera, L.; Blanch, A.R.; Casanovas-Massana, A.; Monleón-Getino, A.; García-Aljaro, C. Traceability of different brands of bottled mineral water during shelf life, using PCR-DGGE and next generation sequencing techniques. *Food Microbiol.* **2019**, *82*, 1–10. [[CrossRef](#)] [[PubMed](#)]
64. Poitelon, J.B.; Joyeux, M.; Welté, B.; Duguet, J.P.; Prestel, E.; Dubow, M.S. Variations of bacterial 16S rDNA phylotypes prior to and after chlorination for drinking water production from two surface water treatment plants. *J. Ind. Microbiol. Biotechnol.* **2010**, *37*, 117–128. [[CrossRef](#)] [[PubMed](#)]
65. Jalili, F.; Trigui, H.; Guerra Maldonado, J.F.; Dorner, S.; Zamyadi, A.; Shapiro, B.J.; Terrat, Y.; Fortin, N.; Sauvé, S.; Prévost, M. Can Cyanobacterial Diversity in the Source Predict the Diversity in Sludge and the Risk of Toxin Release in a Drinking Water Treatment Plant? *Toxins* **2021**, *13*, 25. [[CrossRef](#)] [[PubMed](#)]
66. Pei, H.; Xu, H.; Wang, J.; Jin, Y.; Xiao, H.; Ma, C.; Sun, J.; Li, H. 16S rRNA Gene Amplicon Sequencing Reveals Significant Changes in Microbial Compositions during Cyanobacteria-Laden Drinking Water Sludge Storage. *Environ. Sci. Technol.* **2017**, *51*, 12774–12783. [[CrossRef](#)] [[PubMed](#)]
67. Douterelo, I.; Husband, S.; Loza, V.; Boxall, J. Dynamics of biofilm regrowth in drinking water distribution systems. *Appl. Environ. Microbiol.* **2016**, *82*, 4155–4168. [[CrossRef](#)]
68. Egorov, A.I.; Birkenhauer Best, J.M.; Frebis, C.P.; Karapondo, M.S. Occurrence of *Aeromonas* spp. in a random sample of drinking water distribution systems in the USA. *J. Water Health* **2011**, *9*, 785–798. [[CrossRef](#)]
69. van der Wielen, P.W.J.J.; van der Kooij, D. Nontuberculous mycobacteria, fungi, and opportunistic pathogens in unchlorinated drinking water in the Netherlands. *Appl. Environ. Microbiol.* **2013**, *79*, 825–834. [[CrossRef](#)]
70. Collado, L.; Kasimir, G.; Perez, U.; Bosch, A.; Pinto, R.; Saucedo, G.; Huguet, J.M.; Jose, M. Occurrence and diversity of *Arcobacter* spp. along the Llobregat River catchment, at sewage effluents and in a drinking water treatment plant. *Water Res.* **2010**, *44*, 3696–3702. [[CrossRef](#)]
71. Boers, S.A.; Jansen, R.; Hays, J.P. Understanding and overcoming the pitfalls and biases of next-generation sequencing (NGS) methods for use in the routine clinical microbiological diagnostic laboratory. *Eur. J. Clin. Microbiol. Infect. Dis.* **2019**, *38*, 1059–1070. [[CrossRef](#)] [[PubMed](#)]